Evolution of high-energy particle distribution in SNRs

Siming Liu and Houdun Zeng

Purple Mountain Observatory

The 8th EASW, Daejeon, Korea

Outline

* Background
* Motivation and model description
* Results and discussion
* Conclusions

Background

Supernova remnants (SNRs) have been proposed as the dominant contributor to galactic cosmic rays (Baade & Zwicky 1934).

1、SNRs have enough total power
 10%, 3 per century, CR density
(1ev/cm^3)；

2、 Direct evidences:

Radio emission (1948)
— GeV electrons

Non-thermal X-ray emission
 (1995)
— TeV electrons

 π^0 bump (2013)W44,IC443,W51C
— GeV protons

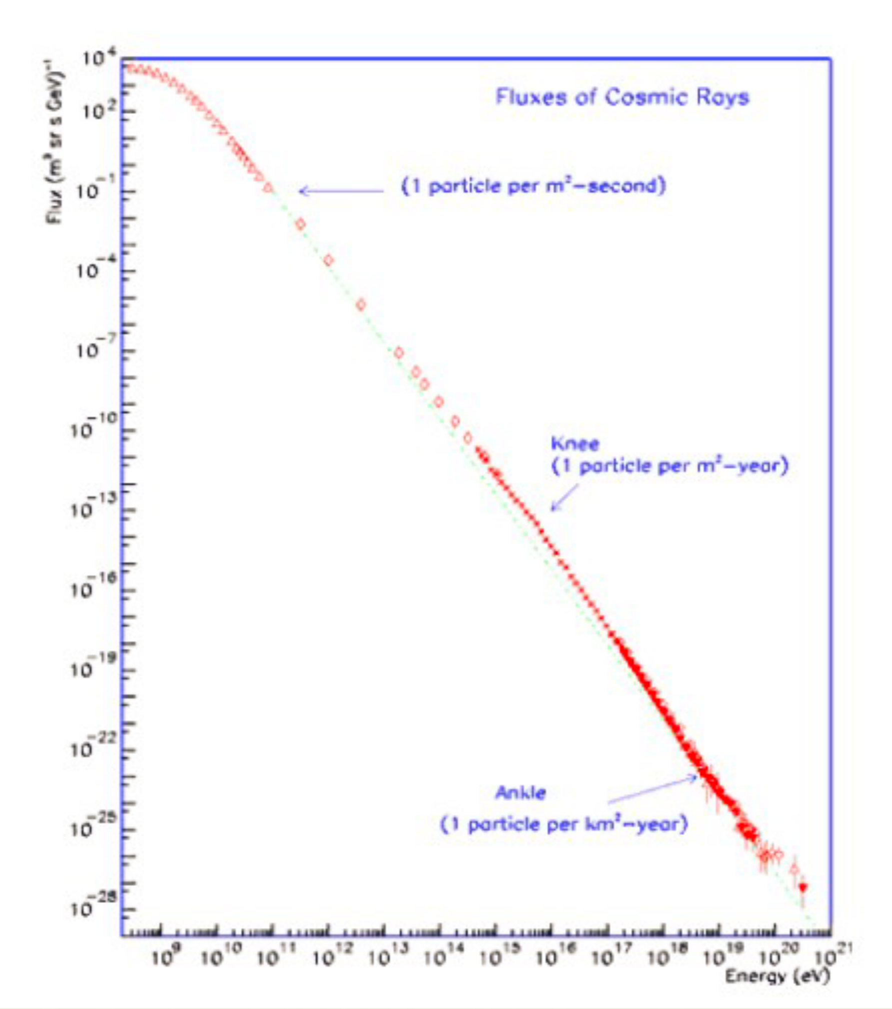

Background

standard theory of shock predicts p=2.0

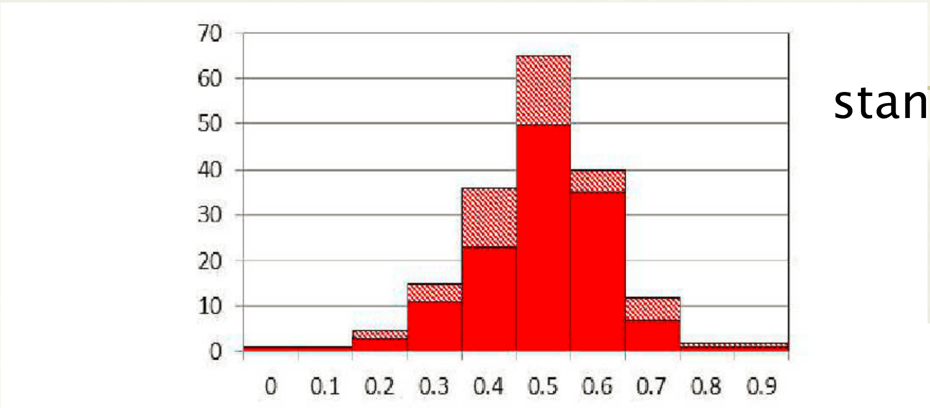

Fig. 6 Histogram of spectral indices of shell-type Galactic SNRs as extracted from Green (2014). Th bars correspond to firm spectral index determination, while the shadowed ones to SNRs with un spectral indices

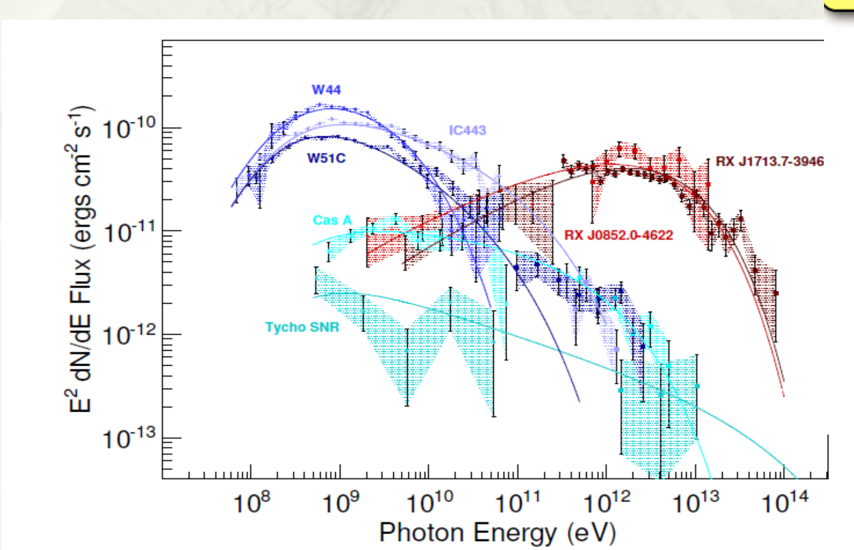

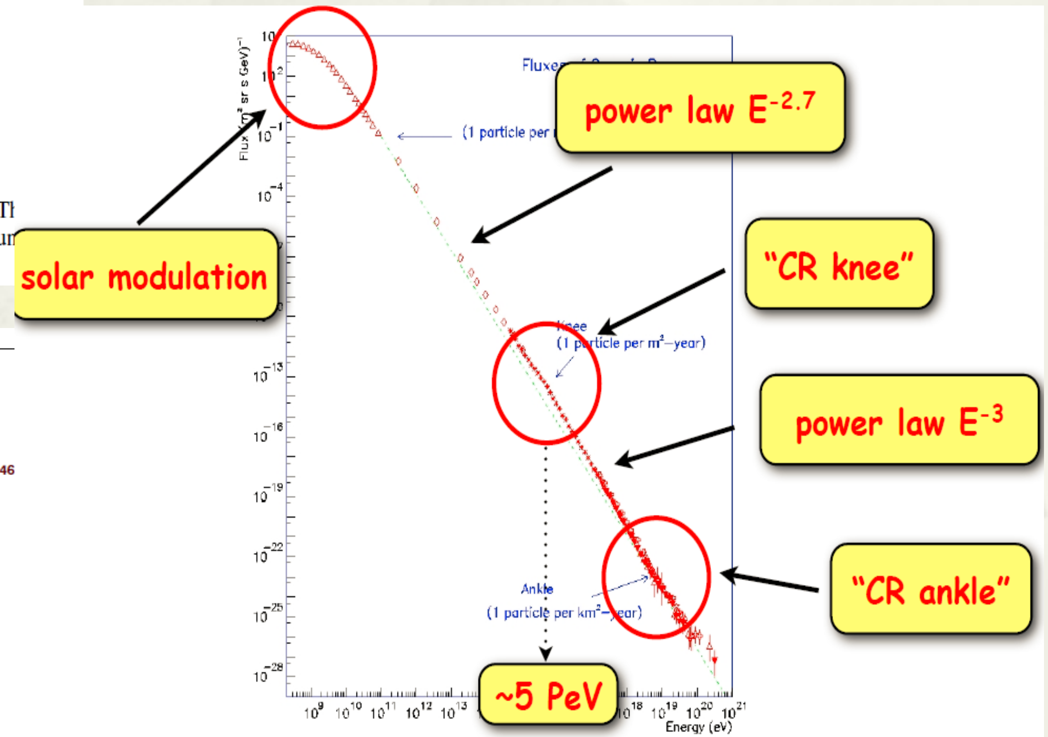

Background

CR spectral → Particles distribution

Yuan et al. 2012

SNRs' SED

$$q_f(R,z) \propto \left(\frac{R}{R_\odot}\right)^{\alpha} \exp\left[-\frac{\beta(R-R_\odot)}{R_\odot}\right] \exp\left(-\frac{|z|}{z_s}\right),$$

$$q(p) \propto \begin{cases} p^{-\alpha_1}, & p < p_{\rm br}, \\ p^{-\alpha_2}, & p \geq p_{\rm br}, \end{cases}$$

$p_{\rm br}c = 6$ GeV

$\alpha_1 = 1.80, \ \alpha_2 = 2.52$

Injection Power :
Proton ~ 3e48 erg/year
Electron ~ 4e46 erg/year

3 SNRs/100 yrs with 1e50 erg protons and 1e48 erg electrons For each SNR.

10% efficiency for type Ia SNRs with a kinetic energy of 1e51ergs

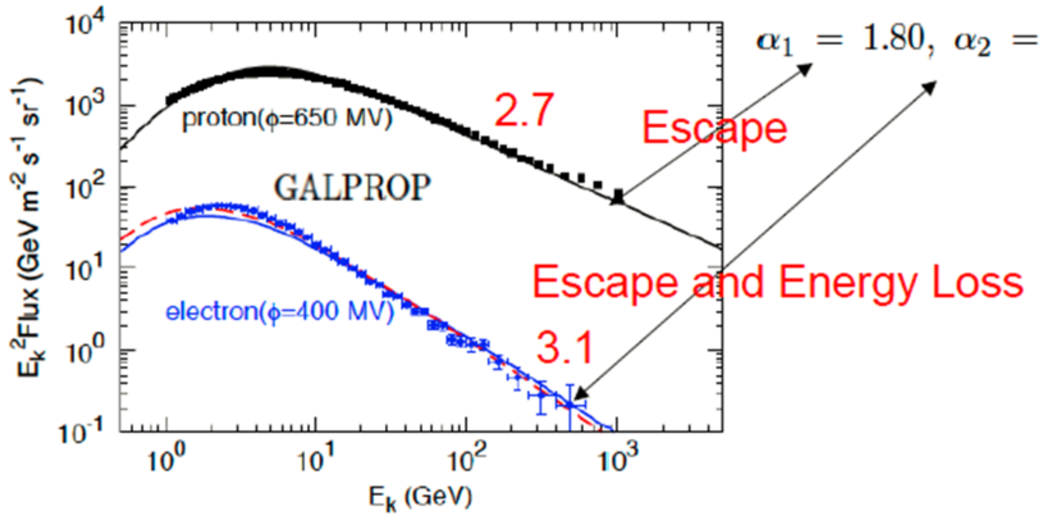

FIG. 1.— The expected fluxes of CR protons and electrons at the Earth, for the same spectral shape of the injected particles, compared with the PAMELA observational data (Adriani et al. 2011a,b). We adopt two parameter settings to calculate the electron spectrum: for solid line the magnetic field is the canonical one adopted in GALPROP and $K_{ep} \approx 1.3\%$; for dashed line the magnetic field is two times larger and $K_{ep} \approx 1.9\%$.

Yuan et al. 2012

n=0.01

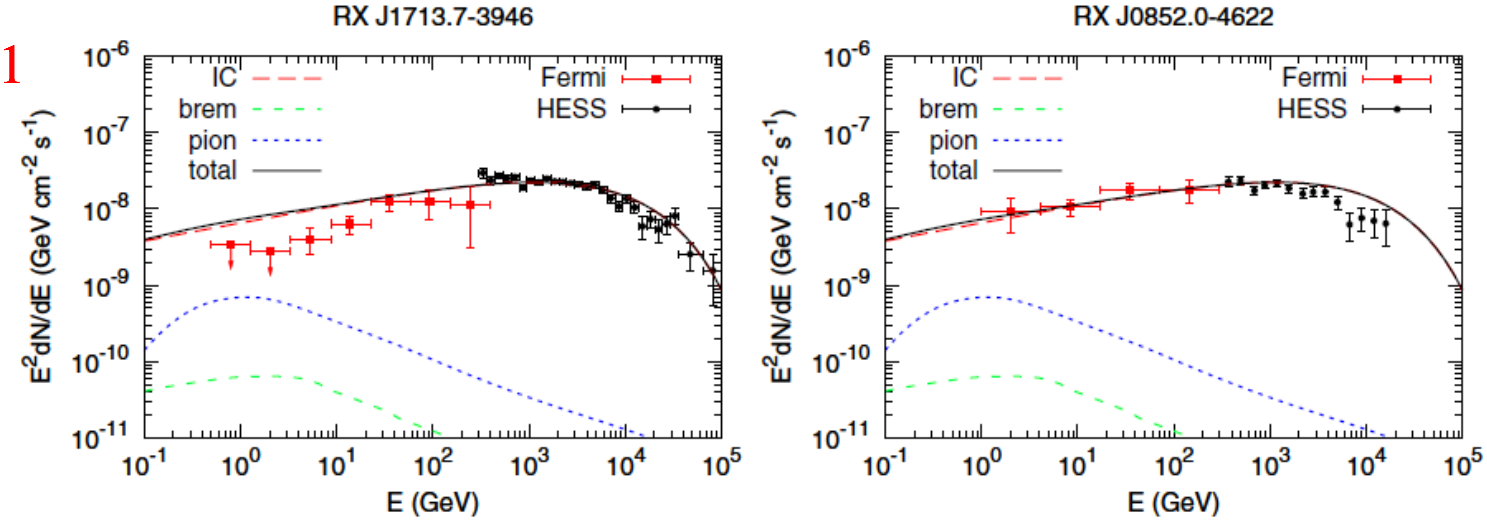

Figure 2. Expected γ-ray spectra for SNRs RX J1713.7−3946 (left) and RX J0852.0−4622 (right). The gas density is adopted to be $n = 0.01$ cm^{-3}. References of the observational data—RX J1713.7−3946: *Fermi* (Abdo et al. 2011), HESS (Aharonian et al. 2007b); RX J0852.0−4622: *Fermi* (Tanaka et al. 2011), HESS (Aharonian et al. 2007a).

n=1.0

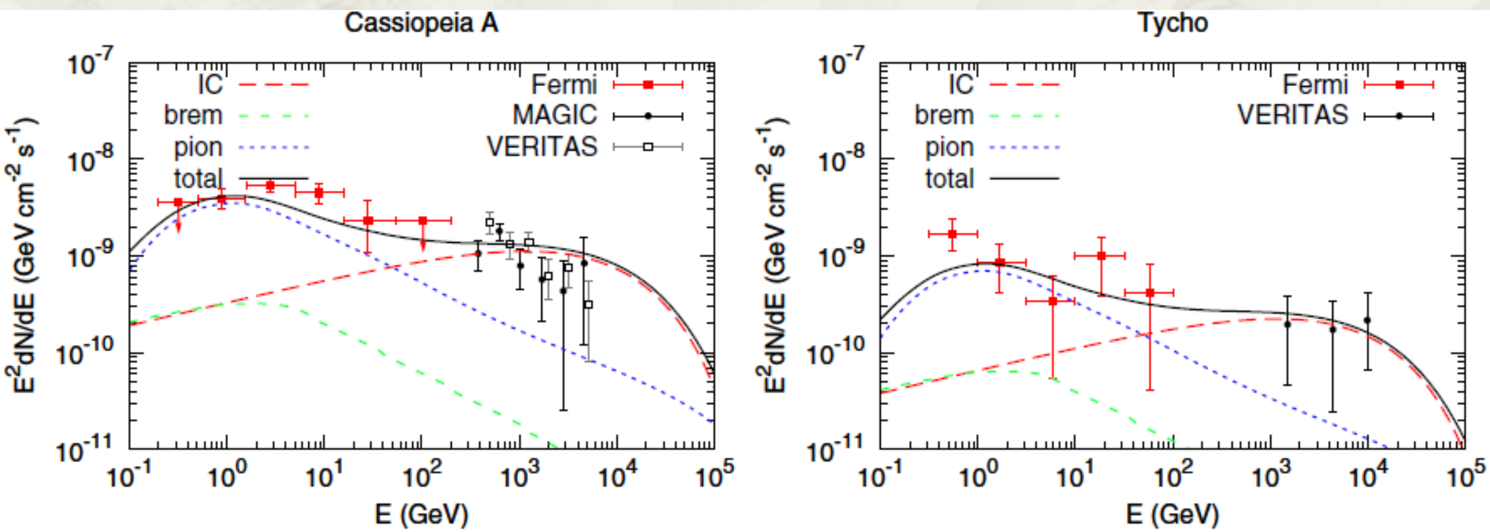

Figure 3. Same as Figure 2, but for Cassiopeia A (left) and Tycho (right). The gas density is adopted to be $n = 1$ cm^{-3}. References of the observational data—Cassiopeia A: *Fermi* (Abdo et al. 2010b), MAGIC (Albert et al. 2007b), VERITAS (Acciari et al. 2010); Tycho: *Fermi* (Giordano et al. 2012), VERITAS (Acciari et al. 2011).

n=100

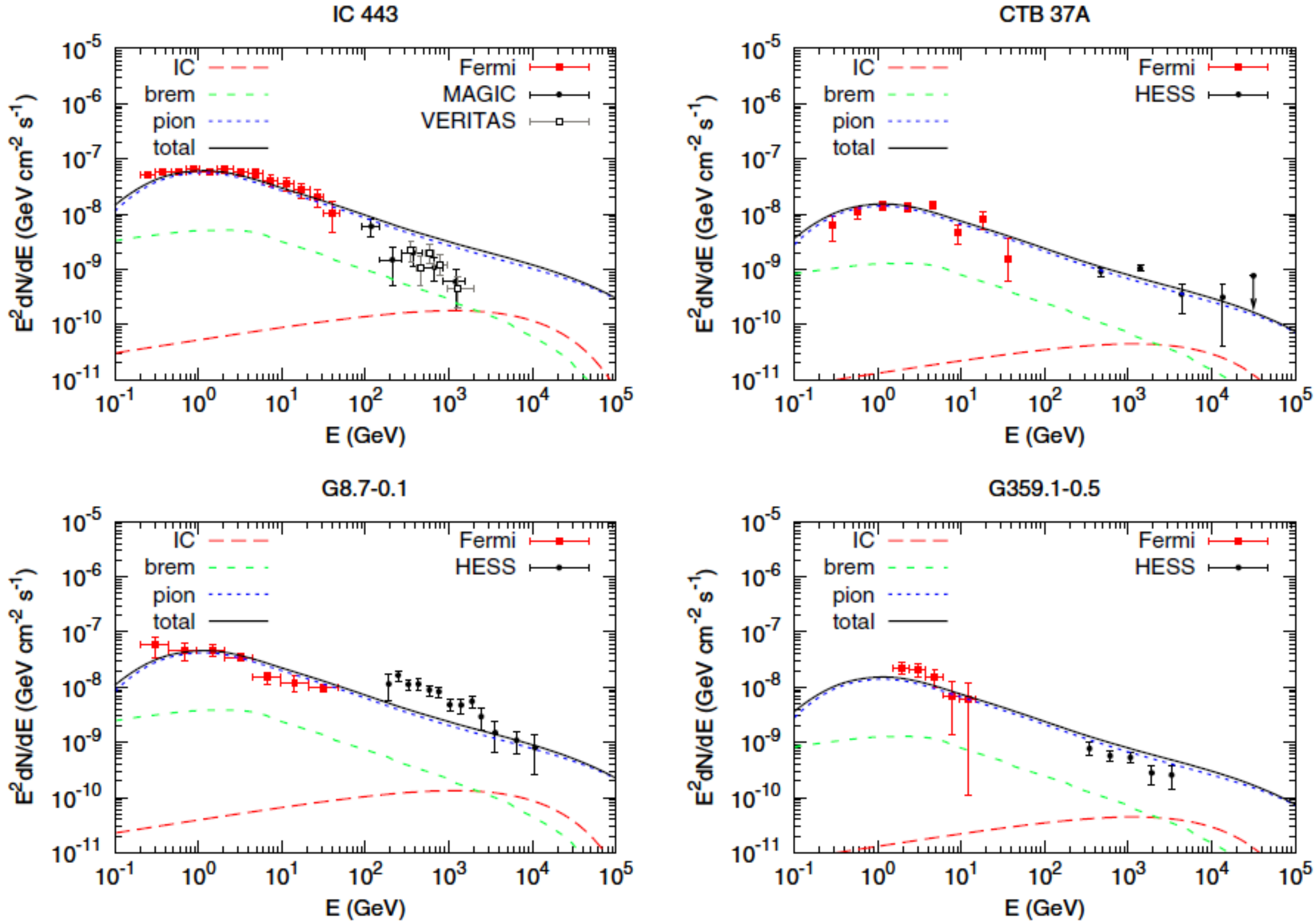

Figure 4. Same as Figure 2, but for SNR–MC interacting systems. The gas density is adopted to be $n = 100\,\mathrm{cm}^{-3}$. References of the observational data—W28: *Fermi* (Abdo et al. 2010a), HESS (Aharonian et al. 2008c); W41: *Fermi* (Mehault et al. 2011), HESS (Mehault et al. 2011); W49B: *Fermi* (Abdo et al. 2010c), HESS (Brun et al. 2011); W51C: *Fermi* (Abdo et al. 2009), HESS (Fiasson et al. 2009), MAGIC (Carmona et al. 2011); IC 443: *Fermi* (Abdo et al. 2010e), MAGIC (Albert et al. 2007a), VERITAS (Acciari et al. 2009); CTB 37A: *Fermi* (Castro & Slane 2010), HESS (Aharonian et al. 2008a); G8.7-0.1: *Fermi* (Ajello et al. 2012), HESS

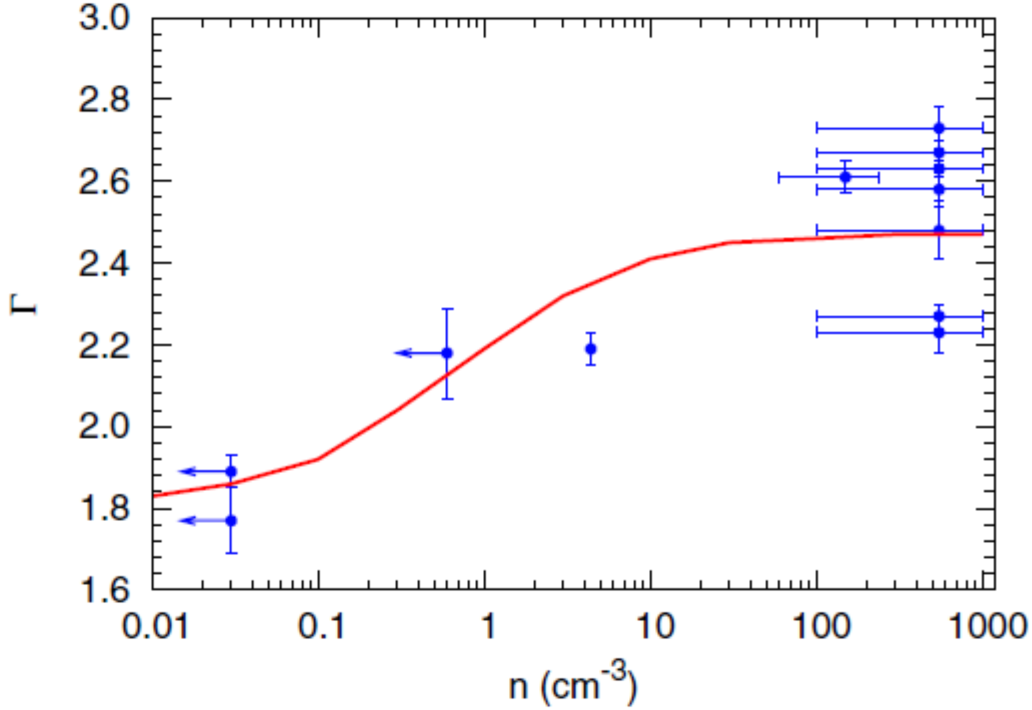

Figure 5. Photon index Γ (between 1 GeV and 1 TeV) vs. the gas density *n* of the 12 SNRs studied in this work. The solid line is the model-expected result.

Gamma-ray spectral variation of SNRs may be due to variation in density of the surrounding environment.

These results can be considered as evidence for the SNR origin of Galactic cosmic rays.

Motivation

SNRs' SED → Particles distribution → CRs

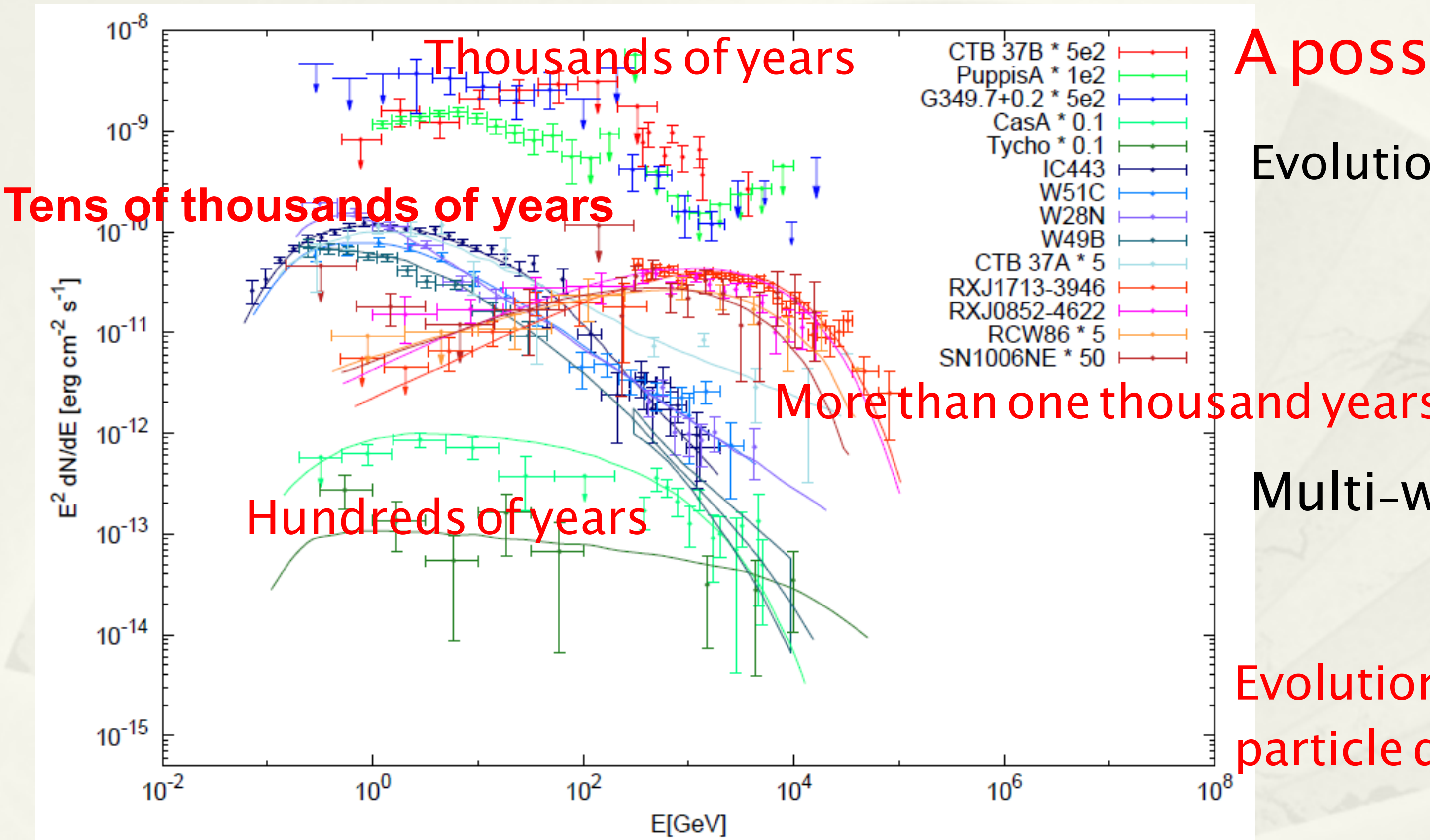

A possible approach:

Evolution of SNRs' SEDs

Multi-wavelength fitting

↓

Evolution of high-energy particle distribution in SNRs

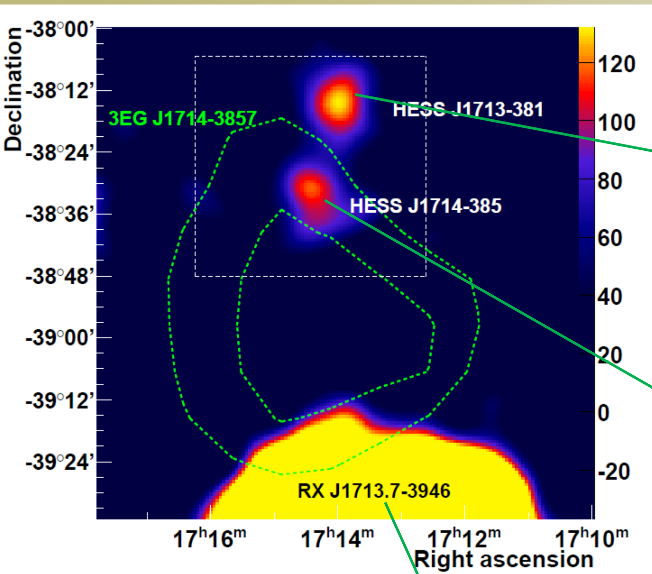

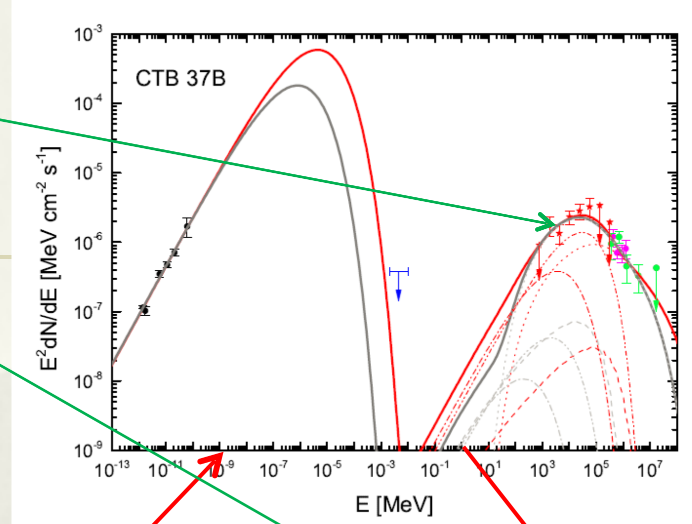

CTB 37B:

~5000 Years

Ebr~400GeV

Both IC and pp contribute to γ-rays

CTB 37A:

>10000 Years Ebr~2GeV

pp dominates γ-rays

RX J1713.7-3946

1600 Years Ebr~1TeV

IC dominates γ-rays

The evolution of SNRs' SEDs

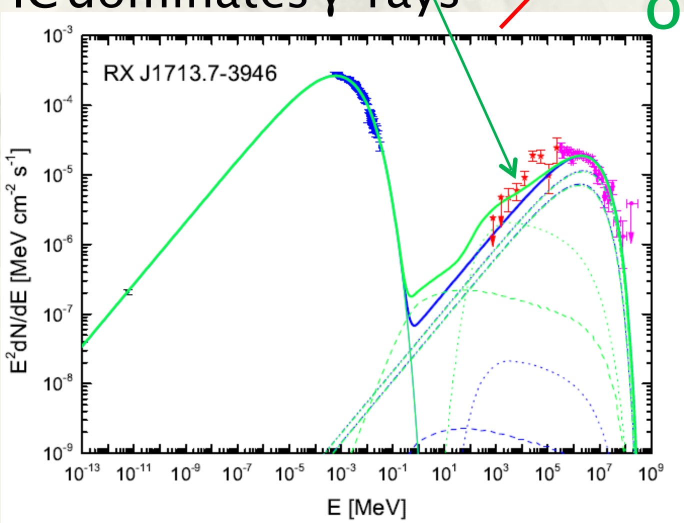

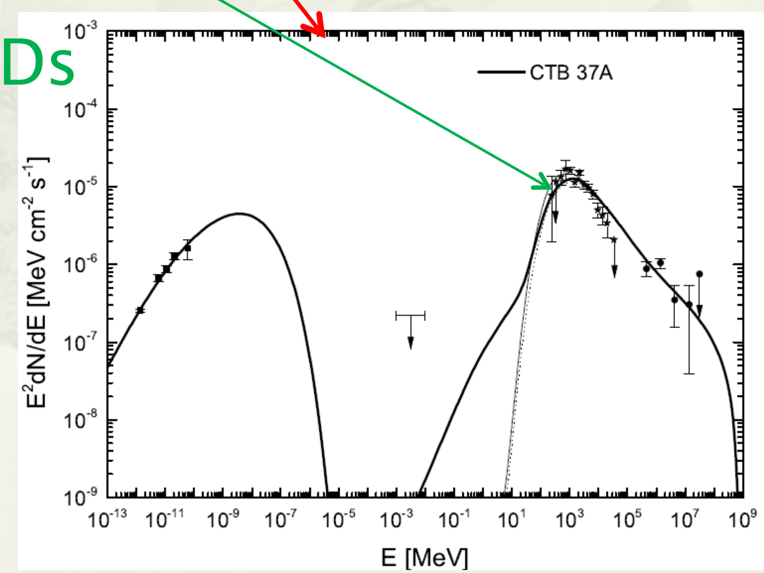

Zeng, H. et al. 2017, ApJ, 834, 153

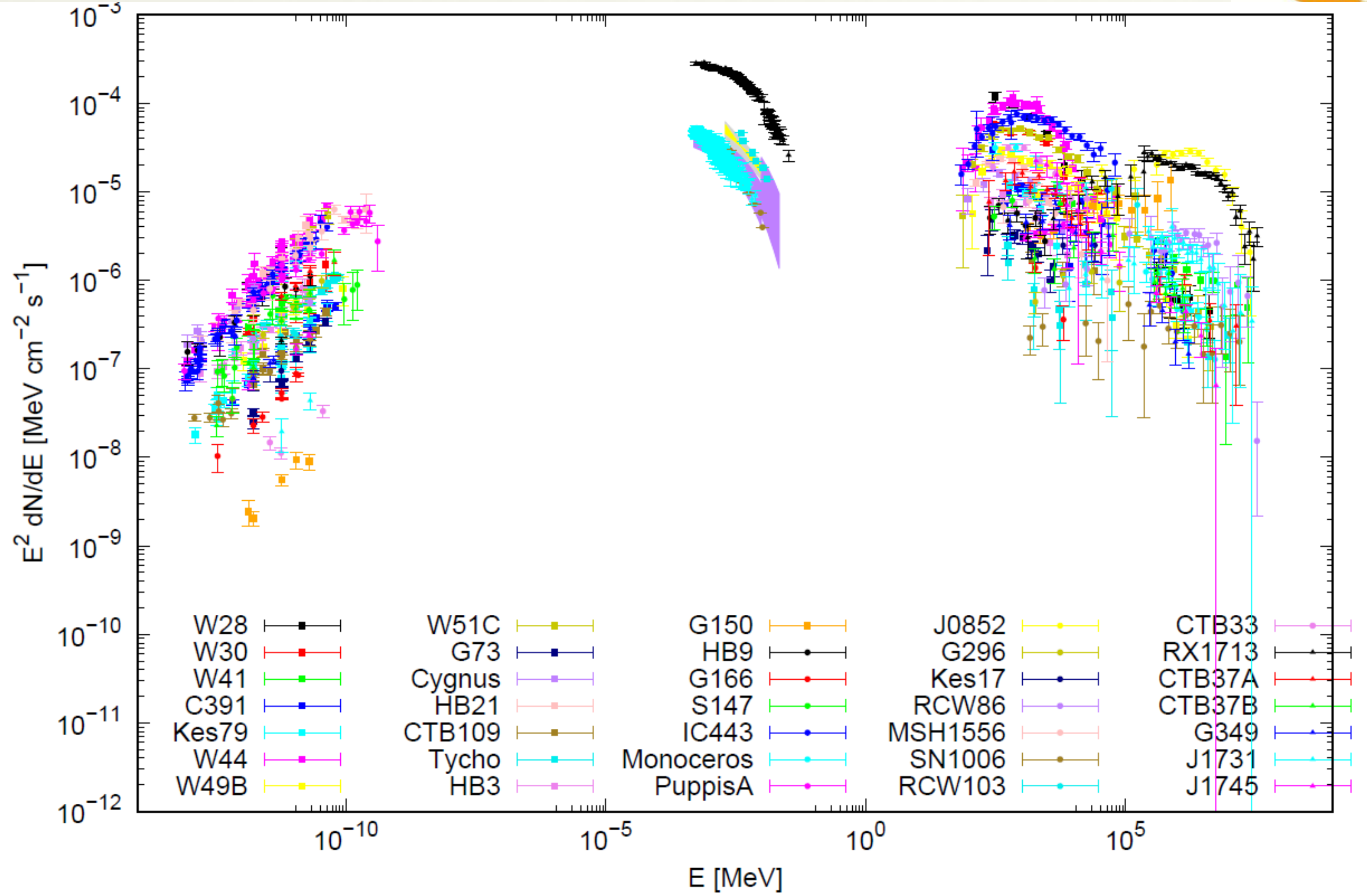

35 SNRs have been selected, 6 X-ray, 16 TeV data

We normalize the flux at100 GeV to 1 x 10^{-5} MeV cm^{-2} s^{-1} by a power-law fit to the spectrum from 1 GeV to 300 GeV to better demonstrate the spectral evolution.

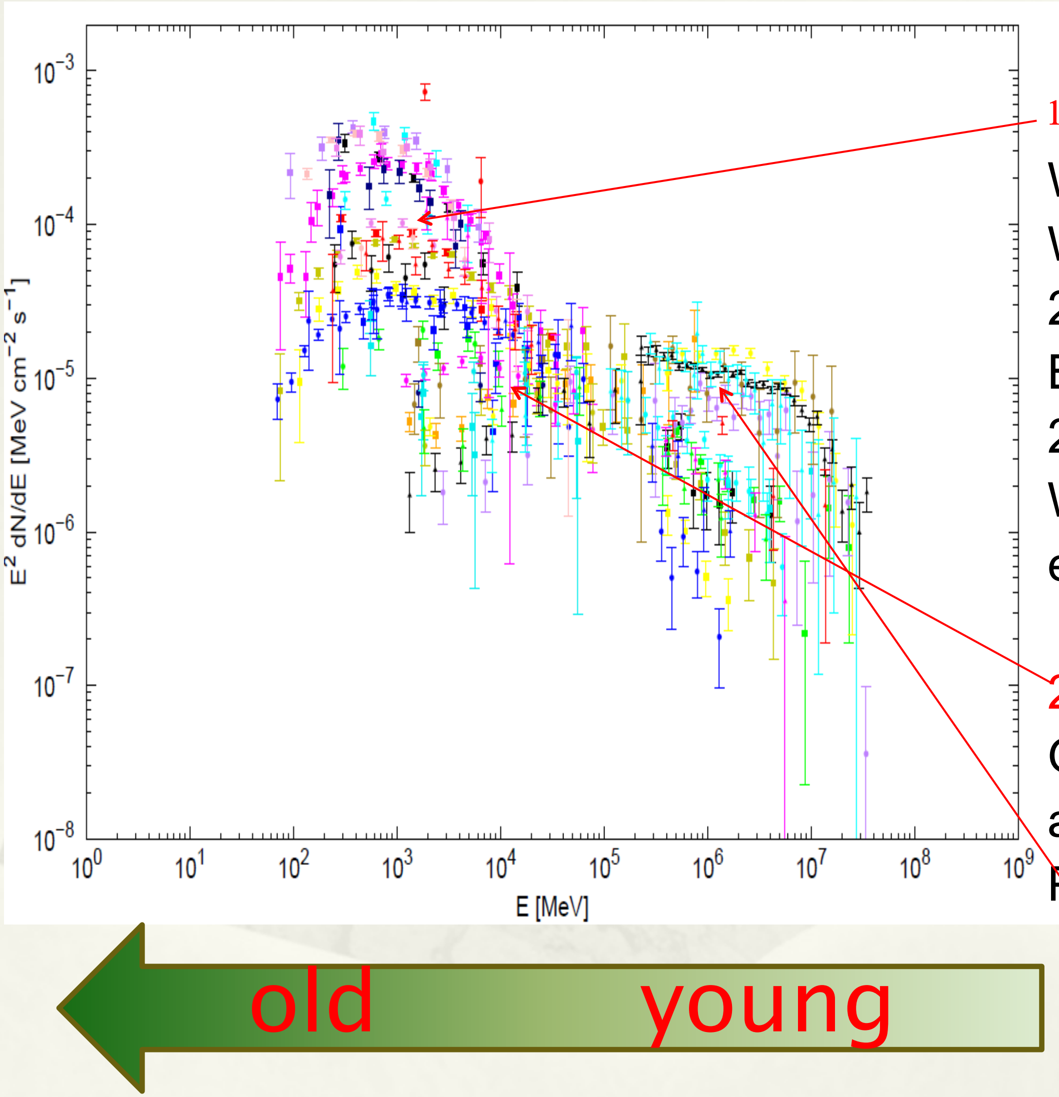

Break energy

1–20GeV:

W28 (Abdo et al. 2010a), W51C (Abdo et al. 2009; Aleksic et al. 2012), W49B (Abdo et al. 2010c; Brun et al. 2011), IC 443(Acciari et al. 2009; Ackermann et al. 2013) W41 (Aharonian et al. 2006b; Castro et al. 2013) and so.

20-200GeV:

G349.7+0.2(Hess Collaboration et al. 2015), CTB 37B(Xin et al.2016), Puppis A (Xin et al. 2017)

1TeV:

RX J1713.7-3946(Hess Collaboration et al. 2017)

A model for broken power-laws in SNRs

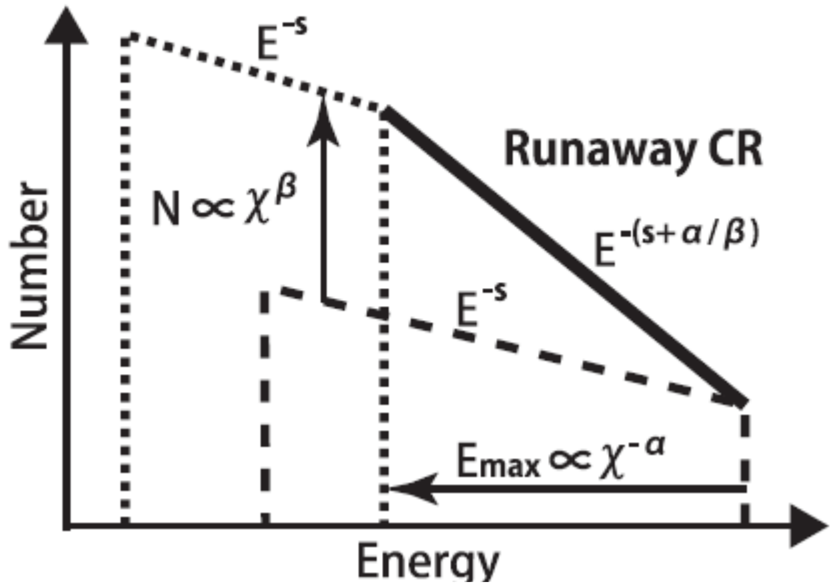

The Astrophysical Journal Letters, 729:L13 (5pp), 2011 March 1

COSMIC-RAY HELIUM HARDENING

Yutaka Ohira and Kunihito Ioka

Mon. Not. R. Astron. Soc. 427, 91–102 (2012) doi:10.1111/j.

Escape of cosmic-ray electrons from supernova remnants

Yutaka Ohira,[1★] Ryo Yamazaki,[1] Norita Kawanaka[2] and Kunihito Ioka[3,4]

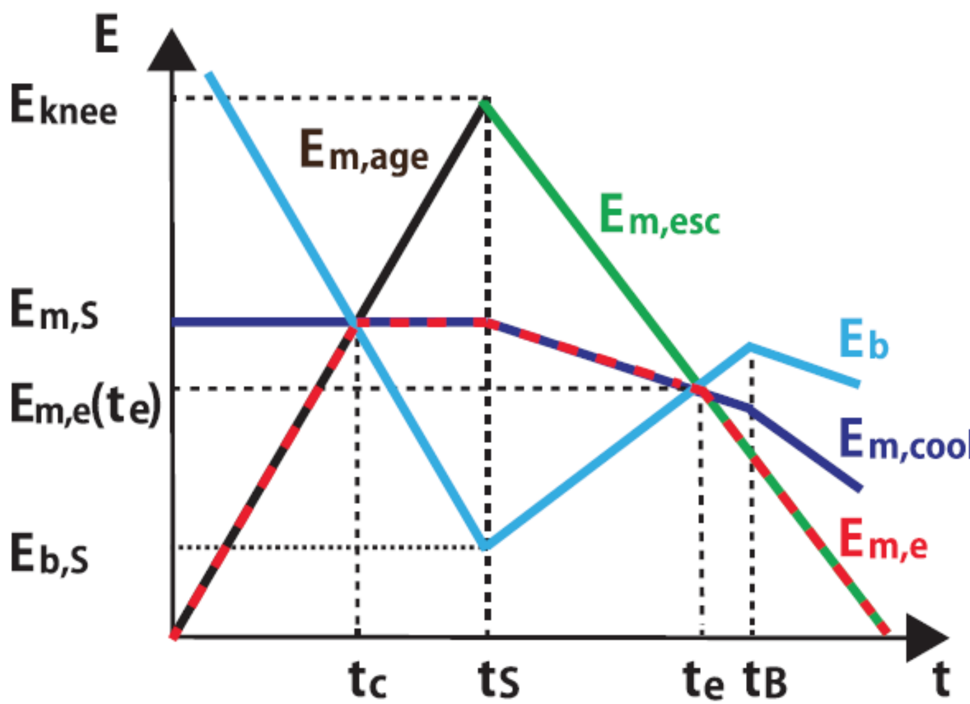

Hα observations

Tycho

Young with wider precursor for higher energy acceleration

Cygnus loop old

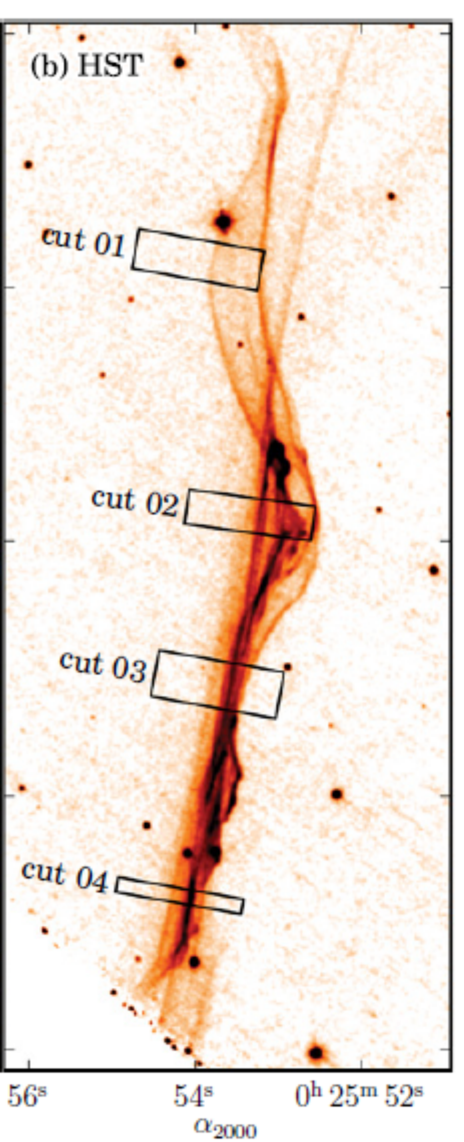

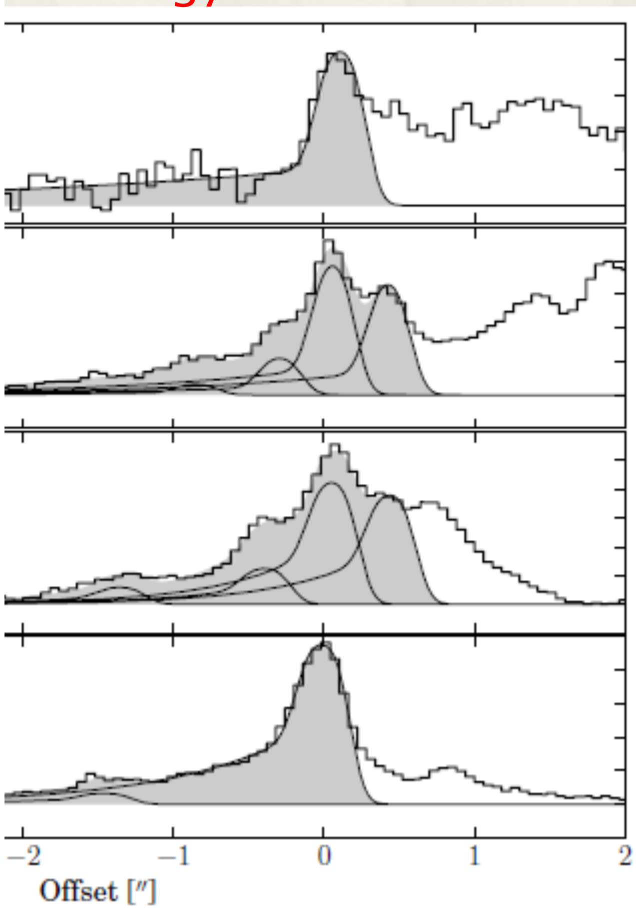

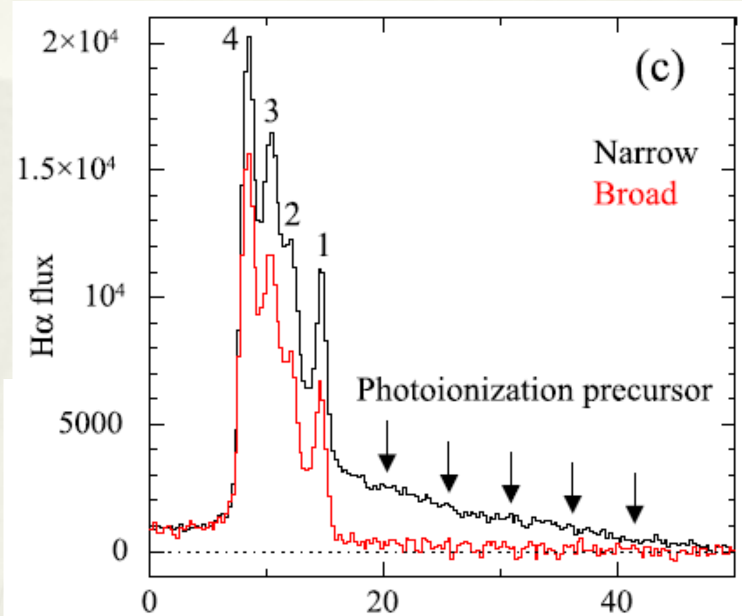

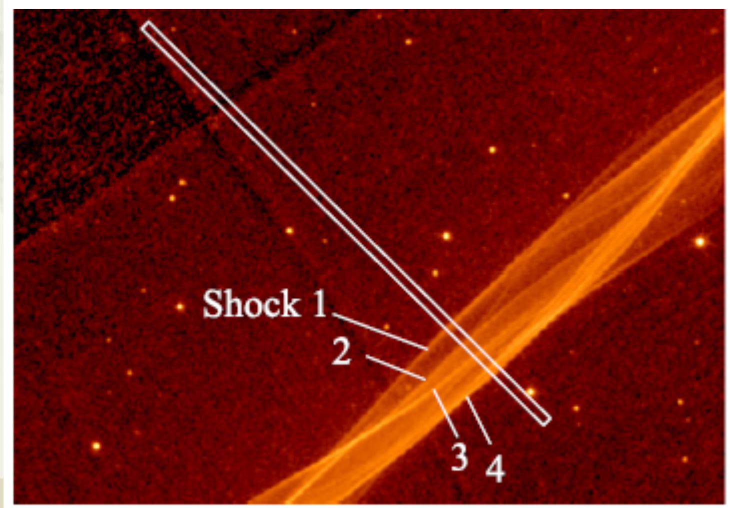

Model description

a simple one-zone model

1. The distribution of particles： "i" represents e or p

$$N(P_i) = N_{0,i}\exp(-\frac{P_i}{P_{i,cut}})\begin{cases} P_i^{-\alpha} & \text{if} \quad P_i < P_{\rm br} \\ P_{i,\rm br}P_i^{-(\alpha+1)} & \text{if} \quad P_i \geq P_{\rm br} \end{cases},$$

2. Kep=0.01, and both leptonic (Synch, Brem and IC) and hadronic (pp) emissions are considered in our fitting.
3. For comparison, the same background photon field is assumed for all SNRs (CMB and IR).
4. Distance, Age, Shock velocity, The gas density from literature

$$\frac{P_{\rm e,cut}}{\rm GeV/c} = 1.25\times10^6(\frac{T_{\rm age}}{\rm Year})^{-1}(\frac{B}{100\mu \rm G})^{-2}$$

In this model, 5 free parameters： , , , , (if need),

MCMC method is applied to constrain these model parameters.

SNR Name	Other Name	Radiu pc	Distance Kpc	Age kyr	n cm^{-3}	V_{shock} Km/s	The data of observations				References
							Radio	X-ray	GeV	TeV	
G006.4−00.1	W28	∼ 13	∼ 2.0	40(33-150)	∼ 100	60-80	✓		✓	✓	[1-4]
G008.7−00.1	W30	∼ 26	∼4.0	25(15-28)	∼ 100	530-750	✓		✓		[5][6]
G023.3−00.3	W41	∼ 19	∼ 4.2	∼ 100	∼ 10	110	✓	T	✓	✓	[7][8]
G031.9−00.0	3C 391	∼ 7	∼ 7.2	∼ 4	∼ 300	620-730	✓		✓		[9-12]
G033.6+00.1	Kes 79	∼ 9.6	∼ 7.0	∼ 4.4-6.7	∼ 3(1-5)	400 ± 5	✓		✓		[13-15]
G034.7-00.0	W44	∼ 12.5	∼ 3.0	∼ 20	∼ 200	100-150	✓		✓		[16-18]
G043.3-00.2	W49B	∼ 5	∼ 10	∼ 5.7(5-6)	∼ 700	∼ 400	✓		✓	✓	[19][20]
G049.2-00.7	W51C	∼ 18	∼ 4.3	∼ 30	∼ 10	∼ 100	✓	T	✓	✓	[21-24]
G073.9+00.9		∼ 16/5.2	∼ 4.0/1.3	∼ 11-12	∼ 10	∼ 200-300	✓	T	✓		[25][26]
G074.0-08.5	Cygnus loop	∼ 16	∼ 0.54	∼ 14	∼ 5.0	240-330	✓		✓		[27-30]
G089.0-04.7	HB21	∼ 26	∼ 1.7	∼ 40(36 or 45)	∼ 15	∼ 125	✓		✓		[31-35]
G109.1-0.1	CTB109	∼ 16	∼ 3.1	∼ 9.0(9.0-9.2)	∼ 1.1	∼ 230 ± 5	✓	T	✓		[36][37]
G120.1-01.4	Tycho	∼ 3.3	∼ 3.0	∼ 0.44	∼ 10/0.3	4600-4800	✓	✓	✓	✓	[38][39]
G132.7-00.3	HB3	∼ 26.4	∼ 2.2	∼ 30.0	∼ 2.0	303-377	✓		✓		[40-42]
G150.3+04.5		∼ 9.4	∼ 0.40	∼ 1.5(0.5-5)	∼ 1.0	?	✓		✓		[43]
G160.9-02.6	HB9	∼ 15	∼ 0.8	5.3(4-7)	∼ 0.1	∼ 740	✓	T	✓		[44][45]
G166.0+04.3		∼ 26	∼ 4.5	24.0	∼ 0.01	∼ 680	✓		✓		[46][47]
G180.0+01.7	S147	∼ 38	∼ 1.3	30(20-10)	∼ 250(100-500)	∼ 500	✓		✓		[48][49]
G189.1-03.0	IC 443	∼ 11	∼ 1.5	∼ 30	∼ 140	60-100	✓		✓	✓	[50-52]
G205.5+0.5	Monoceros	∼ 63.36	∼ 1.98	∼ 30	∼ 3.6	∼ 50	✓		✓		[53-55]
G260.4-03.4	Puppis A	∼ 15	∼ 2.2	4.45(3.75-5.20)	∼ 4.0	700-2500	✓		✓	T	[56-59]
G266.2-01.2	RX J0852-4622	∼ 13	∼ 0.75	2.7(1.7-4.3)	∼ 3.8	∼ 3000	✓	✓	✓	✓	[60][61]
G296.5+10.0		∼ 26	∼ 2.1	∼ 10.0	∼ 13.0	∼ >35	✓		✓		[62][63]
G304.6-00.1	Kes 17	∼ 10	∼ 10	4.2(2-5.2)	∼ 10	150-200	✓		✓		[64][65]
G315.4-02.3	RCW 86	∼ 15	∼ 2.5	∼ 1.8	∼ 0.1-2.0	700-2000	✓	✓	✓	✓	[66-68]
G326.3-01.8	MSH 15-56	∼ 22.2	∼ 4.1	∼ 10.0(10-16.5)	∼ 0.1/1.0	500-860	✓		✓		[67][69][70]
G327.6+14.6	SN 1006 (NE)	∼ 9.0	∼ 2.2	∼ 1.0	∼ 0.085	3200-5800	✓	✓	✓	✓	[71][72]
G332.4-00.4	RCW 103	∼ 5	∼ 3.3	∼ 2.0	∼ 10	∼ 1100	✓		✓		[73-75]
G337.0-00.1	CTB 33	∼ 2.55	∼ 11.0	∼ 5.0	∼ 60	?	✓		✓		[76-78]
G347.3-00.5	RX 1713.7-3946	∼ 10	∼ 1.0	∼ 1.6	∼ 0.01	∼ 5000	✓	✓	✓	✓	[82-84]
G348.5+00.1	CTB 37A	∼ 10	∼ 7.9	∼ 30	∼ 100	75-100	✓	T	✓	✓	[85-89]
G348.7+00.3	CTB 37B	∼ 20	∼ 13.2	∼ 5	∼ 10/0.5	∼ 800	✓	T	✓	✓	[88-91]
G349.7+00.2		∼ 3.3	∼ 11.5	∼ 2.8	∼ 35.0	700-900	✓	T	✓	✓	[92-95]
G353.6-00.7	Hess J1731-347	∼ 14.0	∼ 3.2	∼ 2-6	∼ 0.01	∼ 2100	✓	✓	✓	✓	[96][97]
G359.1-00.5	Hess J1745-303	∼ 16.0	∼ 4.6	∼ 70	∼ 100	∼ 300	✓	T	✓	✓	[98-101]

Note—[1]Kaspi et al. (1993), [2]Abdo et al. (2010), [3]Bohigas et al. (1983), [4]Velázquez et al. (2002), [5]Finley & Oegelman (1994), [6]Ajello et al. (2012), [7]Tian et al. (2007), [8]Castro et al. (2013), [9]Chen et al. (2004), [10]Radhakrishnan et al. (1972), [11]Su et al. (2014a), [12]Wilner et al. (1998), [13]Giacani et al. (2009), [14]Zhou et al. (2016), [15]Auchettl et al. (2014), [16]Wolszczan et al. (1991), [17]Yoshiike et al. (2013), [18]Reach & Rho (2000), [19]Zhou & Vink (2017), [20]Brogan & Troland (2001), [21]Koo et al. (1995), [22]Aleksić et al. (2012), [23]Tian & Leahy (2013), [24]Koo & Moon (1997), [25]Lozinskaya et al. (1993), [26]Pavlović et al. (2013), [27]Levenson et al. (1998), [28]Blair et al. (2005), [29]Hester et al. (1994), [30]Salvesen et al. (2009), [31]Mavromatakis et al. (2007),[32]Koo & Heiles (1991), [33]Byun et al. (2006), [34]Pivato et al. (2013), [35]Koo & Heiles (1991), [36]Castro et al. (2012), [37]Sánchez-Cruces et al. (2018), [38]Hayato et al. (2010), [39]Cassam-Chenaï et al. (2007), [40]Lazendic & Slane (2006), [41]Routledge et al. (1991), [42]Gosachinskii (2005), [43]Cohen (2016), [44]Leahy & Aschenbach (1995), [45]Leahy & Tian (2007), [46]Burrows & Guo (1994), [47]Landecker et al. (1989), [48]Chatterjee et al. (2009), [49]Katsuta et al. (2012), [50]Olbert et al. (2001), [51]Welsh & Sallmen (2003), [52]Su et al. (2014b), [53]Leahy et al. (1986), [54]Zhao et al. (2018), [55]Xiao & Zhu (2012), [56]Becker et al. (2012), [57]Reynoso et al. (2003), [58]Arendt et al. (2010), [59]H. E. S. S. Collaboration et al. (2015b), [60]Katsuda et al. (2008), [61]Slane et al. (2001), [62]Vasisht et al. (1997), [63]Giacani et al. (2000), [64]Gelfand et al. (2013), [65]Hewitt et al. (2009), [66]Helder et al. (2013), [67]Rosado et al. (1996), [68]Bocchino et al. (2000), [69]Temim et al. (2013), [70]Yatsu et al. (2013), [71]Winkler et al. (2003), [72]Katsuda et al. (2009), [73]Carter et al. (1997), [74]Caswell et al. (1975), [75]Frank et al. (2015), [76]Sarma et al. (1997), [77]Corbel et al. (1999), [78]Castro et al. (2013), [79]Lemiere et al. (2009), [80]Abramowski et al. (2014), [81]Slane et al. (2010), [82]Wang et al. (1997), [83]Yuan et al. (2011), [84]Fukui et al. (2003), [85]Sezer et al. (2011), [86]Andersen et al. (2011), [87]Reynoso & Mangum (2000), [88]Tian & Leahy (2012), [89]Zeng et al. (2017), [90]Aharonian et al. (2008),[91]Nakamura et al. (2009), [92]Slane et al. (2002), [93]Tian & Leahy (2014), [94]Ergin et al. (2015), [95]Lazendic et al. (2005), [96]Tian et al. (2008), [97]H.E.S.S. Collaboration et al. (2011), [98]Ohnishi et al. (2011), [99]Hayakawa et al. (2012), [100]Yusef-Zadeh et al. (2007), [101]Hewitt et al. (2008)

Results and discussion

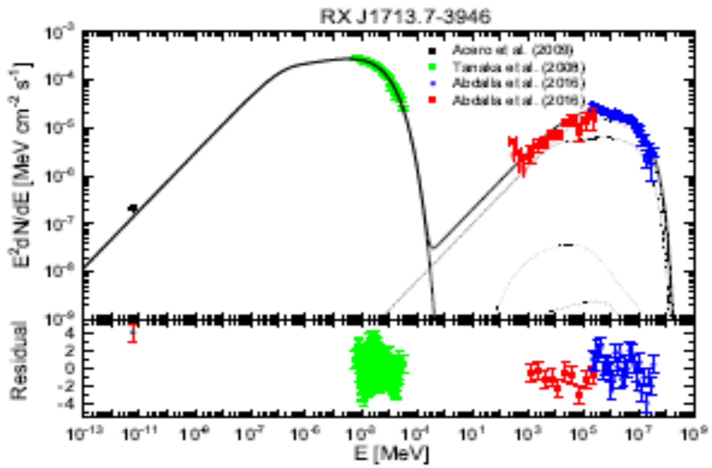

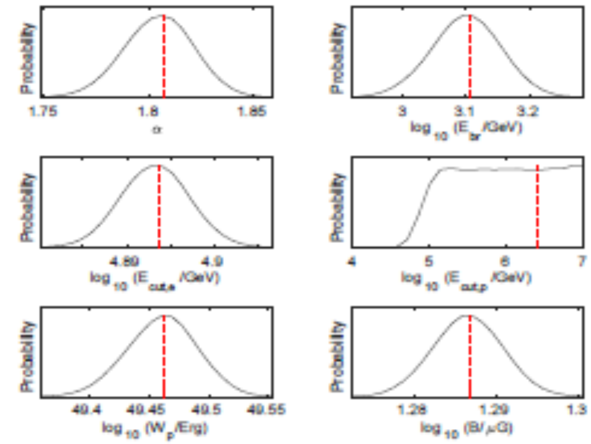

RX J1713.7-3946

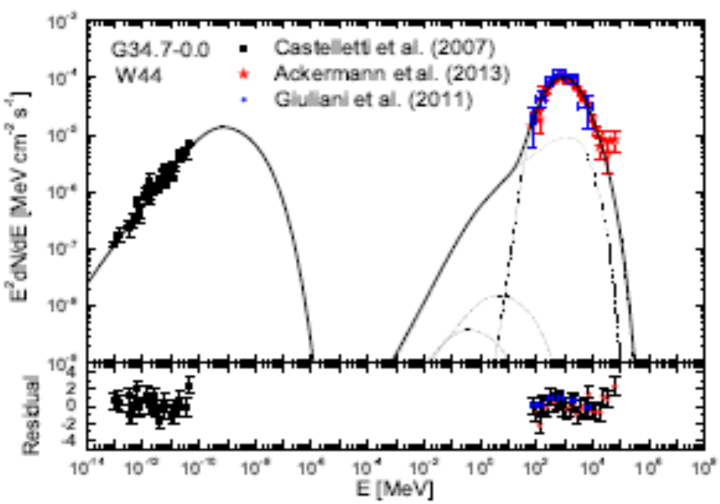

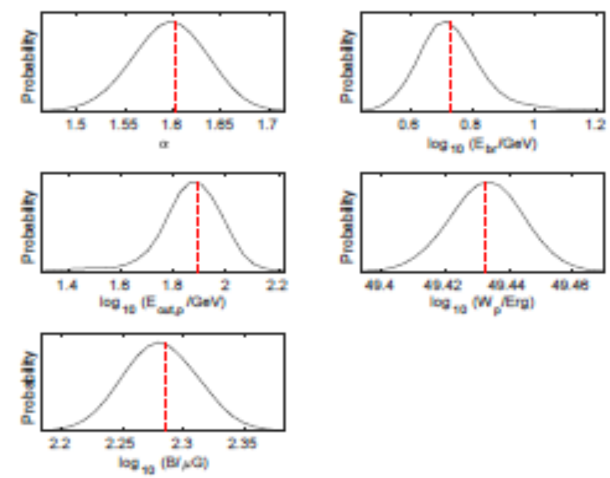

W44

Source Name	α	$\log10 \frac{E_{br}}{GeV}$	$\log10 \frac{E_{e,cut}}{GeV}$	$\log10 \frac{E_{p,cut}}{GeV}$	$\log10 \frac{B}{\mu G}$	$\log10 \frac{W_p}{erg}$	$\frac{W_B}{W_e}$	$\frac{n}{cm^{-3}}$	$\frac{\chi^2}{NDF}$
W28	$1.76^{+0.03}_{-0.03}$	$0.18^{+0.11}_{-0.11}$	1.63	> 5.72	$1.94^{+0.04}_{-0.04}$	$49.36^{+0.02}_{-0.02}$	3.0×10^3	100	$\frac{24.3}{10} = 2.43$
W30	$1.63^{+0.10}_{-0.11}$	$0.24^{+0.33}_{-0.38}$	2.06	> 4.29	$1.86^{+0.12}_{-0.13}$	$49.69^{+0.07}_{-0.07}$	736	100	$\frac{6.0}{7} = 0.86$
W41	$1.22^{+0.04}_{-0.04}$	< -0.30	1.37	$4.52^{+0.20}_{-0.20}$	$1.87^{+0.11}_{-0.11}$	$50.21^{+0.05}_{-0.05}$	464	10	$\frac{12.6}{12} = 1.05$
3C391	$1.99^{+0.05}_{-0.05}$	$1.15^{+0.14}_{-0.14}$	1.86	> 3.81	$2.31^{+0.04}_{-0.04}$	$49.03^{+0.03}_{-0.03}$	619	300	$\frac{37.1}{19} = 1.95$
Kes79	$2.11^{+0.05}_{-0.05}$	$0.71^{+0.15}_{-0.15}$	2.89	> 4.32	$1.74^{+0.04}_{-0.04}$	$49.47^{+0.04}_{-0.04}$	28.9	100.0	$\frac{66}{23} = 2.54$
W44	$1.60^{+0.04}_{-0.04}$	$0.73^{+0.09}_{-0.09}$	1.23	$1.87^{+0.11}_{-0.09}$	$2.28^{+0.03}_{-0.03}$	$49.43^{+0.01}_{-0.01}$	1.48×10^3	200	$\frac{44.4}{48} = 0.93$
W49B	$1.47^{+0.04}_{-0.04}$	$-0.21^{+0.23}_{-0.24}$	1.55	$3.70^{+0.13}_{-0.13}$	$2.40^{+0.06}_{-0.06}$	$49.43^{+0.02}_{-0.02}$	235	700	$\frac{18.9}{20} = 1.00$
W51C	$1.56^{+0.02}_{-0.02}$	$0.31^{+0.08}_{-0.08}$	1.64	$4.39^{+0.30}_{-0.29}$	$2.08^{+0.03}_{-0.03}$	$49.83^{+0.01}_{-0.01}$	708	100	$\frac{59.7}{29} = 2.06$
W51C[b]	$1.64^{+0.02}_{-0.02}$	$0.32^{+0.05}_{-0.05}$	1.57	> 5.78	$2.02^{+0.03}_{-0.03}$	$49.79^{+0.01}_{-0.01}$	201	100	$\frac{34.9}{29} = 1.20$
G73.9+0.9[c]	$0.78^{+0.19}_{-0.19}$	$0.96^{+0.09}_{-0.09}$	$0.96^{+0.09}_{-0.09}$	$0.96^{+0.09}_{-0.09}$	$1.57^{+0.05}_{-0.05}$	$49.34^{+0.04}_{-0.04}$	393	10	$\frac{22.4}{13} = 1.72$
Cygnus Loop	$2.01^{+0.05}_{-0.05}$	$0.69^{+0.09}_{-0.09}$	2.85	> 4.09	$1.47^{+0.02}_{-0.02}$	$48.72^{+0.02}_{-0.02}$	232	5.0	$\frac{21.9}{19} = 1.15$
HB21	$1.21^{+0.10}_{-0.10}$	$0.61^{+0.08}_{-0.08}$	$0.73^{+0.07}_{-0.07}$	$0.77^{+0.07}_{-0.06}$	$1.74^{+0.02}_{-0.02}$	$49.42^{+0.01}_{-0.01}$	562	15	$\frac{36.4}{21} = 1.73$
CTB109	$1.94^{+0.09}_{-0.09}$	$2.66^{+0.38}_{-0.81}$	3.28	> 4.82	$1.47^{+0.17}_{-0.20}$	$49.84^{+0.12}_{-0.12}$	19.6	1.1	$\frac{20.9}{8} = 2.61$
Tycho	$2.15^{+0.02}_{-0.02}$	$3.37^{+0.12}_{-0.12}$	$4.14^{+0.08}_{-0.09}$	> 5.04	$2.15^{+0.04}_{-0.05}$	$49.01^{+0.08}_{-0.08}$	23.5	0.3	$\frac{55}{35} = 1.57$
Tycho	$2.16^{+0.02}_{-0.02}$	$3.36^{+0.11}_{-0.11}$	$4.06^{+0.07}_{-0.07}$	> 4.93	$2.29^{+0.04}_{-0.05}$	$48.78^{+0.07}_{-0.07}$	92.2	10.0	$\frac{44}{35} = 1.26$
HB3	$2.07^{+0.10}_{-0.10}$	$0.76^{+0.14}_{-0.14}$	3.50	> 4.57	$1.07^{+0.03}_{-0.03}$	$50.03^{+0.03}_{-0.03}$	7.49	2.0	$\frac{16.8}{18} = 0.93$
G150.3+4.5	$1.73^{+0.22}_{-0.22}$	$2.65^{+0.36}_{-0.42}$	6.04	> 6.37	$0.45^{+0.13}_{-0.13}$	$48.33^{+0.05}_{-0.05}$	1.42	1.0	$\frac{11.5}{12} = 0.96$
HB9	$2.23^{+0.06}_{-0.06}$	$0.89^{+0.12}_{-0.12}$	5.07	> 5.68	$0.67^{+0.04}_{-0.04}$	$50.10^{+0.05}_{-0.05}$	0.16	0.1	$\frac{15.2}{14} = 1.09$
G166.0+4.3[c]	$1.32^{+0.17}_{-0.18}$	1.87	1.87	$1.87^{+0.14}_{-0.15}$	$0.57^{+0.24}_{-0.24}$	$50.92^{+0.26}_{-0.25}$	0.12	0.01	$\frac{6.92}{5} = 1.38$
G166.0+4.3[c]	$1.26^{+0.17}_{-0.18}$	1.18	1.18	$1.18^{+0.16}_{-0.16}$	$1.62^{+0.10}_{-0.10}$	$49.18^{+0.07}_{-0.07}$	717	10.0	$\frac{7.70}{5} = 1.54$
S147	$1.36^{+0.06}_{-0.06}$	$-0.14^{+0.12}_{-0.13}$	0.09	> 3.86	$2.77^{+0.09}_{-0.09}$	$47.71^{+0.05}_{-0.05}$	2.7×10^8	250	$\frac{17.3}{17} = 1.02$
S147	$1.53^{+0.11}_{-0.11}$	$0.51^{+0.12}_{-0.12}$	3.57	> 4.65	$1.03^{+0.05}_{-0.05}$	$49.94^{+0.04}_{-0.04}$	31.6	1.0	$\frac{19.8}{17} = 1.16$
IC 443	$1.38^{+0.03}_{-0.03}$	$0.12^{+0.07}_{-0.07}$	1.35	$3.22^{+0.10}_{-0.10}$	$2.14^{+0.02}_{-0.02}$	$48.96^{+0.01}_{-0.01}$	2.28×10^3	140	$\frac{92.0}{64} = 1.44$
Monoceros Loop	$1.63^{+0.02}_{-0.02}$	$0.74^{+0.11}_{-0.11}$	2.97	> 5.77	$1.31^{+0.03}_{-0.03}$	$50.29^{+0.03}_{-0.03}$	224	3.6	$\frac{42.5}{16} = 1.63$
Puppis A	$2.08^{+0.02}_{-0.02}$	$3.23^{+0.48}_{-0.56}$	2.50	> 4.57	$1.97^{+0.02}_{-0.02}$	$49.53^{+0.04}_{-0.04}$	500	4.0	$\frac{48.8}{30} = 1.46$
RX J0852-4622[d]	$2.21^{+0.04}_{-0.04}$		$4.30^{+0.06}_{-0.06}$	> 5.15	$1.03^{+0.04}_{-0.04}$	$49.61^{+0.05}_{-0.05}$	2.79	0.01	$\frac{27.8}{16} = 1.74$
RX J0852-4622	$1.33^{+0.05}_{-0.05}$	$1.13^{+0.18}_{-0.16}$	$4.38^{+0.06}_{-0.06}$	> 5.15	$1.04^{+0.04}_{-0.04}$	$49.70^{+0.04}_{-0.04}$	2.6	0.01	$\frac{18.6}{15} = 1.24$
G296.5+10.0	$1.86^{+0.08}_{-0.08}$	> 3.75	0.59	> 3.99	$2.73^{+0.13}_{-0.13}$	$48.55^{+0.14}_{-0.14}$	1.15×10^7	13.0	$\frac{4.3}{5} = 0.86$
Kes 17	$2.01^{+0.18}_{-0.17}$	> 3.52	3.03	> 4.20	$1.79^{+0.17}_{-0.17}$	$50.33^{+0.11}_{-0.11}$	7.0	10.0	$\frac{1.06}{2} = 0.53$
RCW 86	$2.26^{+0.02}_{-0.02}$	$3.92^{+0.08}_{-0.09}$	$4.42^{+0.04}_{-0.03}$	> 5.23	$1.44^{+0.02}_{-0.02}$	$49.82^{+0.03}_{-0.03}$	15.3	0.01	$\frac{31.5}{22} = 1.43$
MSH 15-56	$1.43^{+0.14}_{-0.14}$	$2.13^{+0.17}_{-0.20}$	2.40	> 3.06	$1.81^{+0.09}_{-0.08}$	$51.05^{+0.13}_{-0.13}$	34.3	0.1	$\frac{10.1}{7} = 1.44$
MSH 15-56	$1.61^{+0.12}_{-0.12}$	$1.17^{+0.08}_{-0.11}$	3.02	> 3.83	$1.60^{+0.10}_{-0.10}$	$50.75^{+0.06}_{-0.06}$	9.7	1.0	$\frac{8.0}{7} = 1.14$
SN 1006	$2.09^{+0.04}_{-0.04}$	> 4.84	$3.86^{+0.10}_{-0.10}$	> 4.92	$1.77^{+0.05}_{-0.06}$	$48.72^{+0.07}_{-0.07}$	240	0.085	$\frac{49.0}{35} = 1.40$
RCW 103	$2.11^{+0.08}_{-0.08}$	> 3.86	3.90	> 4.87	$1.45^{+0.08}_{-0.08}$	$50.00^{+0.06}_{-0.06}$	0.44	10	$\frac{1.0}{6} = 0.17$
CTB 33	$2.00^{+0.38}_{-0.33}$	$1.41^{+0.56}_{-0.55}$	4.67	> 5.43	$0.87^{+0.08}_{-0.08}$	$50.47^{+0.07}_{-0.07}$	0.001	60	$\frac{9.06}{5} = 1.81$
RX J1713.7-3946[a]	$1.81^{+0.02}_{-0.02}$	$3.10^{+0.05}_{-0.05}$	$4.89^{+0.004}_{-0.004}$	> 5.57	$1.29^{+0.004}_{-0.004}$	$49.46^{+0.03}_{-0.03}$	6.0	0.01	$\frac{445}{240} = 1.85$
CTB 37A	$1.47^{+0.02}_{-0.02}$	$0.36^{+0.19}_{-0.17}$	1.0	> 5.96	$2.40^{+0.12}_{-0.10}$	$49.82^{+0.02}_{-0.02}$	607	100	$\frac{23.4}{16} = 1.46$
CTB 37B	$1.49^{+0.11}_{-0.11}$	$2.40^{+0.33}_{-0.34}$	0.81	> 5.34	$2.84^{+0.15}_{-0.15}$	$50.51^{+0.04}_{-0.04}$	1.04×10^5	10	$\frac{15.6}{14} = 1.11$
CTB 37B	$1.58^{+0.07}_{-0.07}$	$3.06^{+0.19}_{-0.20}$	2.47	> 5.32	$1.97^{+0.06}_{-0.06}$	$51.60^{+0.04}_{-0.04}$	28.3	0.5	$\frac{14.1}{14} = 1.00$
G349.7+0.2	$2.06^{+0.13}_{-0.12}$	$2.82^{+0.30}_{-0.38}$	2.70	> 5.00	$2.00^{+0.12}_{-0.12}$	$50.09^{+0.04}_{-0.04}$	1.30	35	$\frac{5.2}{10} = 0.52$
Hess J1731-347	$1.86^{+0.04}_{-0.04}$	$3.65^{+0.10}_{-0.10}$	$4.27^{+0.02}_{-0.02}$	> 5.19	$1.46^{+0.02}_{-0.02}$	$49.42^{+0.04}_{-0.04}$	45.1	0.01	$\frac{283.9}{322} = 0.88$
Hess J1745-303	$1.64^{+0.04}_{-0.04}$	$0.52^{+0.20}_{-0.18}$	2.03	> 5.37	$1.66^{+0.08}_{-0.08}$	$49.53^{+0.08}_{-0.08}$	167	100	$\frac{3.62}{8} = 0.45$

中国科学院紫金山天文台
PURPLE MOUNTAIN OBSERVATORY, CAS

Results and discussion

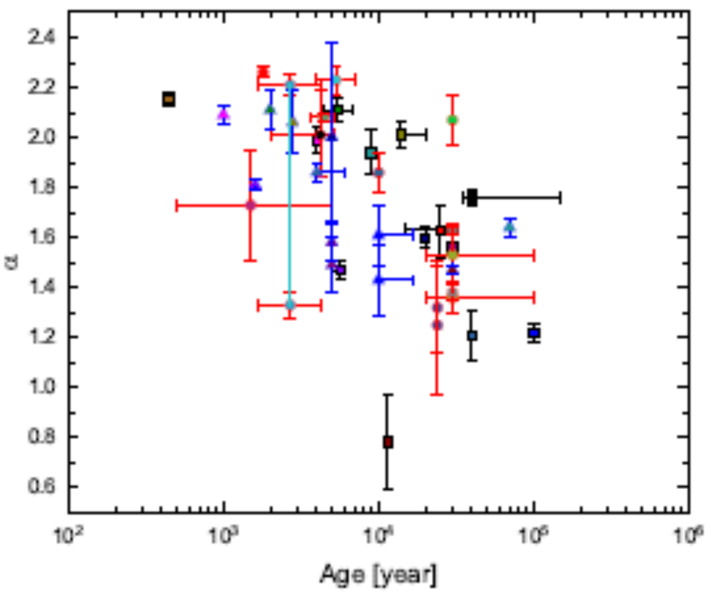

(a)

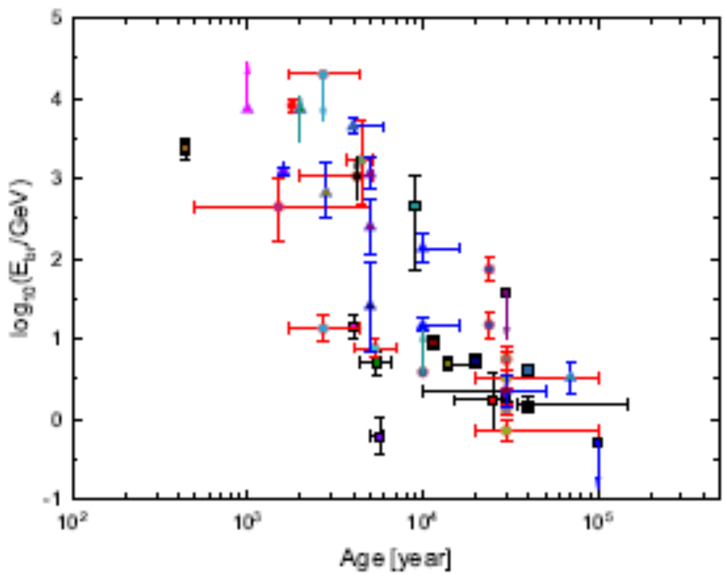

(b)

Figure (a) show there is an inverse correlation between the low-energy spectra index and age, and the spectral become harder with aging of SNRs. This result agrees with the observational fact that the radio spectrum harden with aging of SNRs (e.g. Dubner & Giacani (2015))..

Figure (b): The break energy of particle distribution decreases with the age of SNRs, which may be related to the gradual weakening of shock waves with aging in SNRs and agree with the particle acceleration model with proposed by Ohira et al. (see also Zhang et al.2017)

Results and discussion

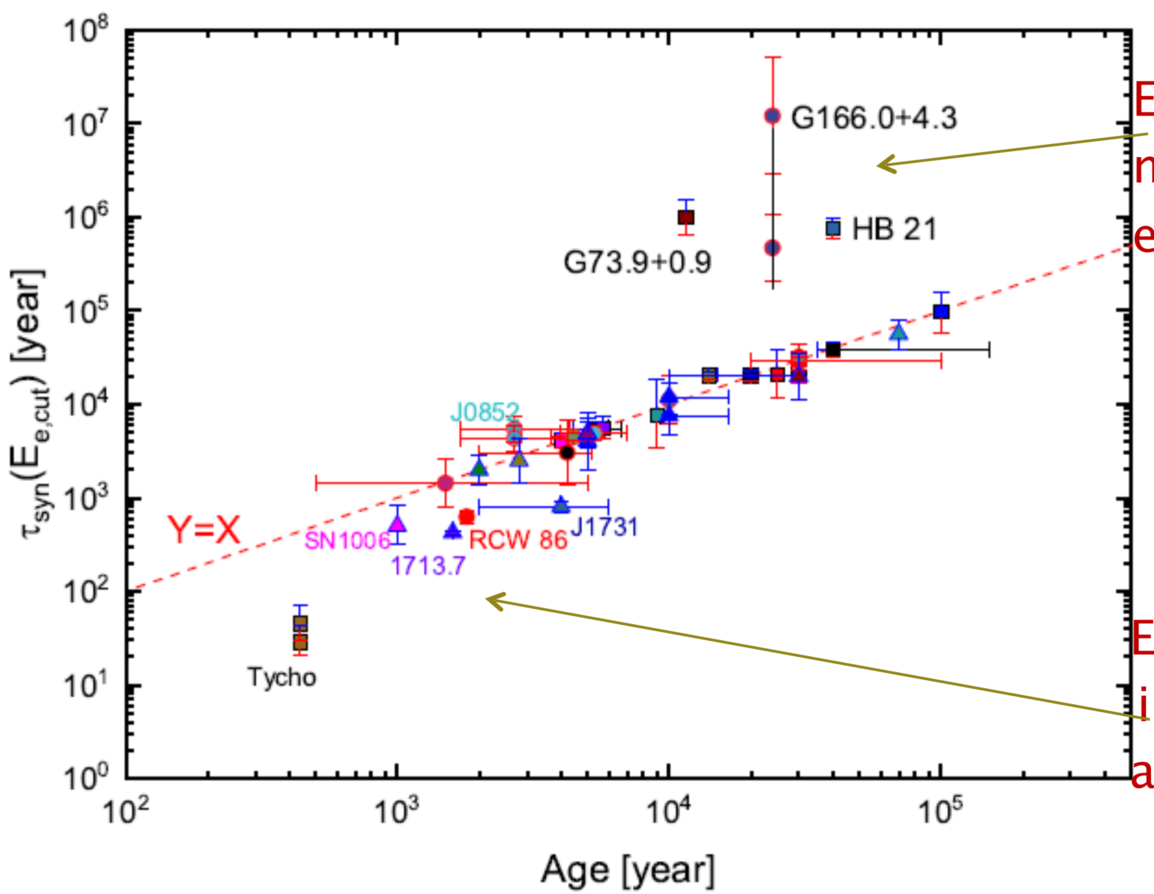

(d)

Energy loss timescale > Age may suggest escape of highest energy particles from SNRs.

Energy loss timescale < Age implying continuous particle acceleration in the interior of SNR

For most middle-age SNRs, the energy loss timescale of electrons at the high-energy cutoff is approximately equal to the age of SNRs, implying quenching of high-energy electron acceleration (Ohira et al).

Results and discussion

中国科学院紫金山天文台
PURPLE MOUNTAIN OBSERVATORY, CAS

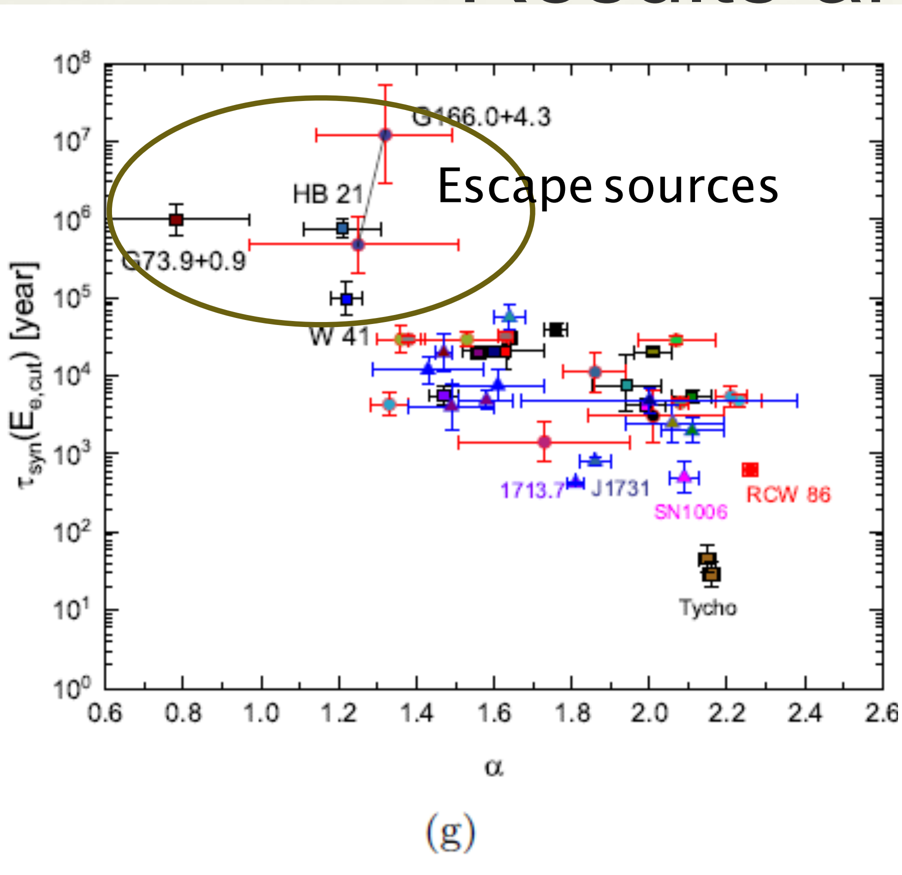

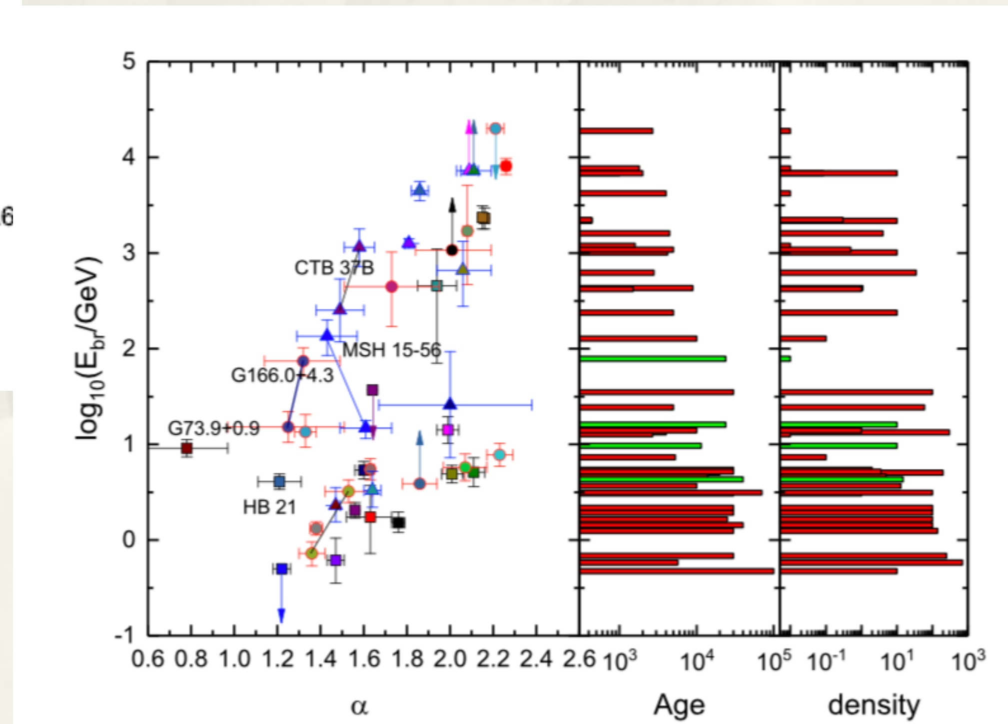

Results and discussion

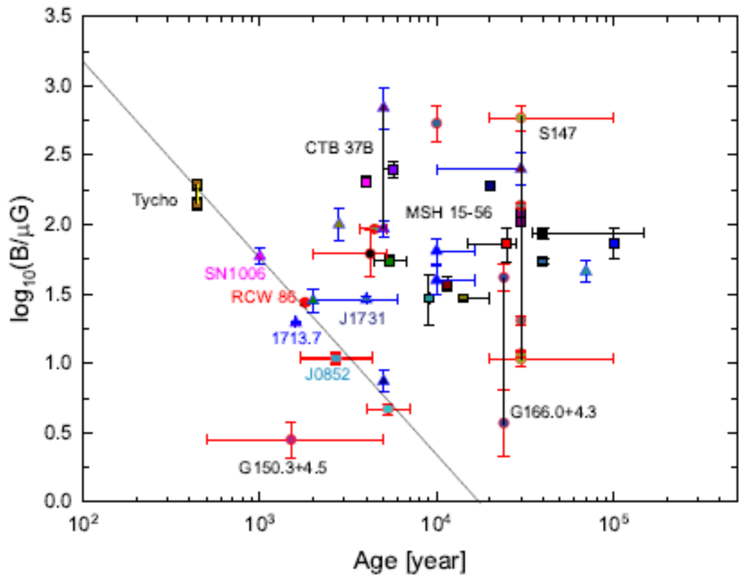

(e)

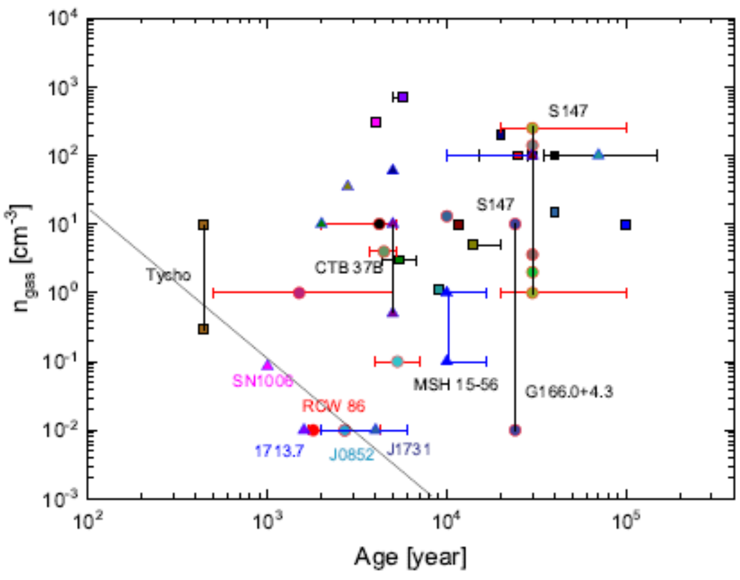

(f)

These two figures respectively show that the relationship between the magnetic field, the gas density and the age of SNRs. The results show there are no correlation between them, but an anti-correlation may be existence for several young shell-type SNRs, consistent with evolution in wind bubbles.

Results and discussion

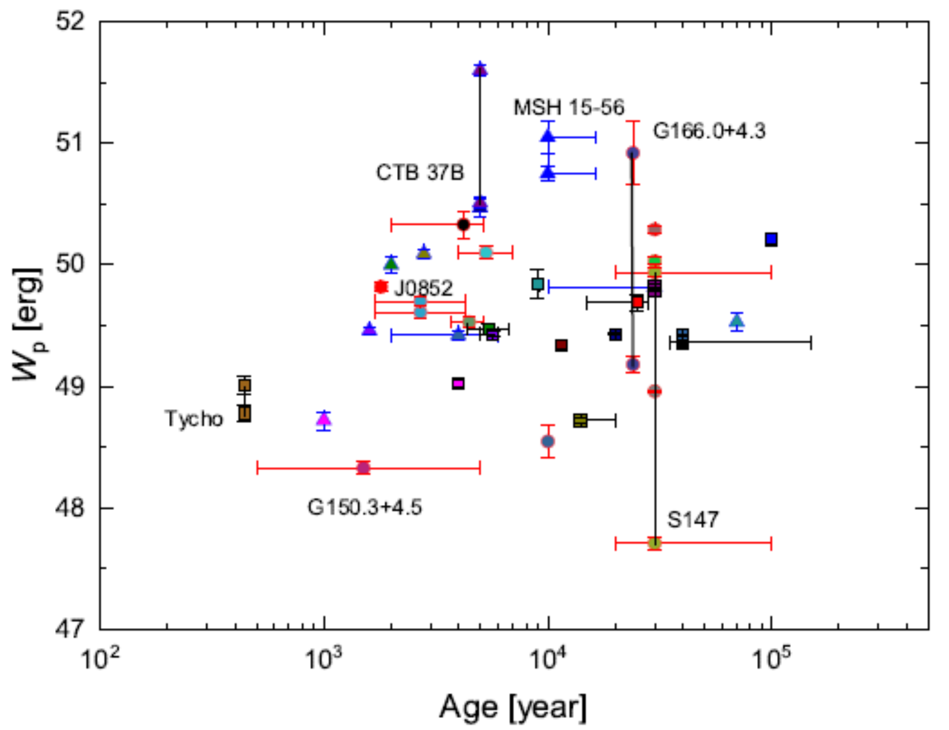

(c)

Figure (c): The total energy of particles for most of SNRs are greater than erg which can be regarded as the lower limit of the cosmic rays produced by SNRs and also supports that SNRs are the sources of Galactic cosmic rays .

Results and discussion

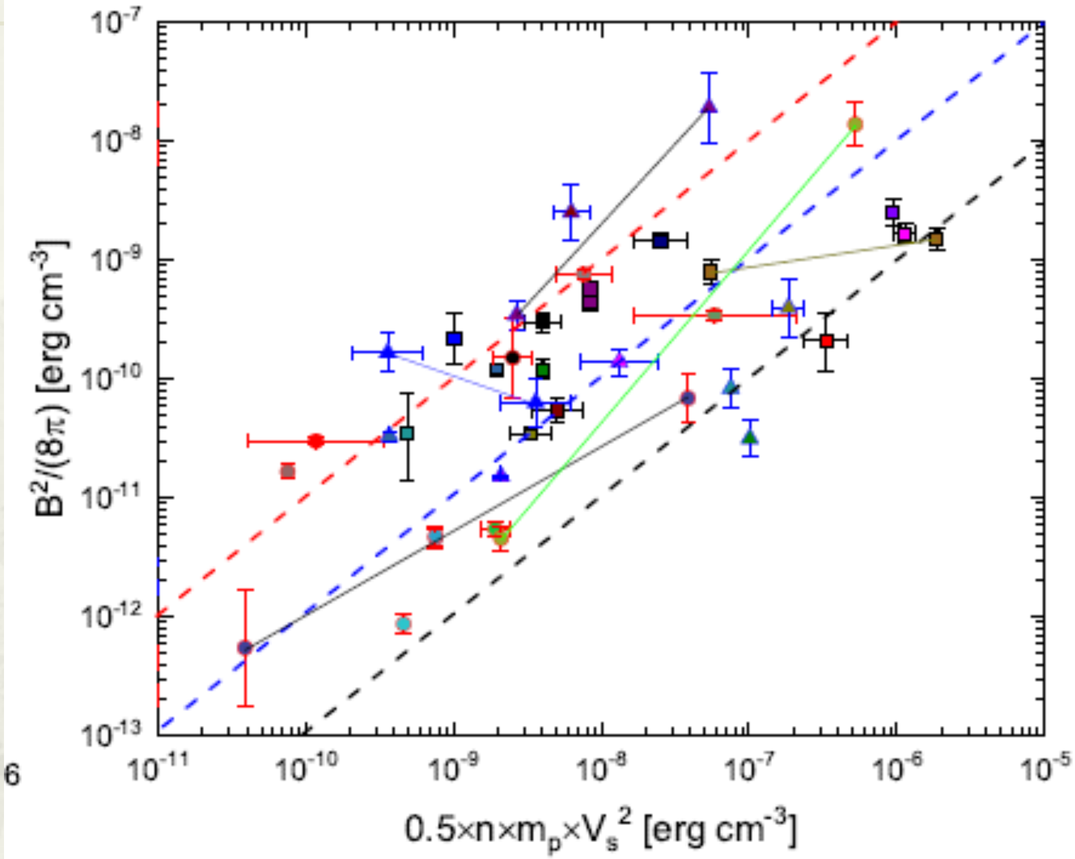

(h)

Discussion

(Possible relation between Particles and CRs spectrum)

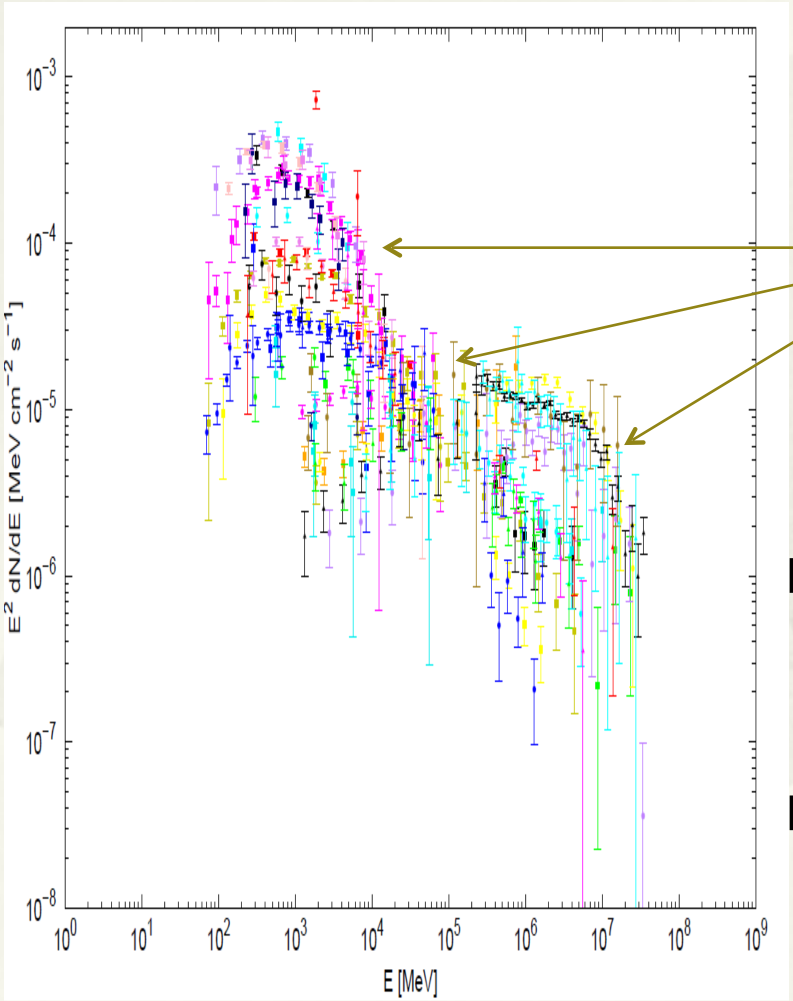

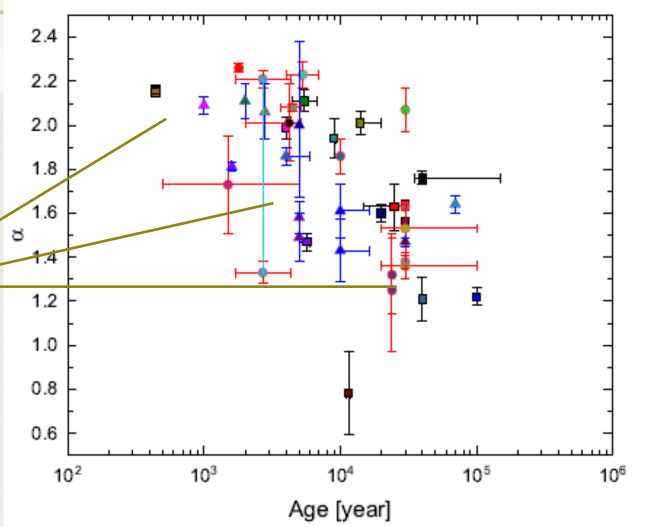

For young SNRs：

For old SNRs：

propagation effect 0.4

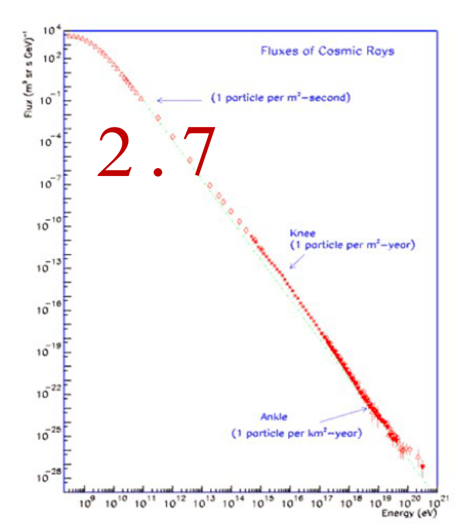

The Astrophysical Journal Letters, 844:L3 (5pp), 2017 July 20
https://doi.org/10.3847/2041-8213/aa7de1

CrossMark

Anomalous Distributions of Primary Cosmic Rays as Evidence for Time-dependent Particle Acceleration in Supernova Remnants

Yiran Zhang[1,2], Siming Liu[1,2], and Qiang Yuan[1,2]
[1] Key Laboratory of Dark Matter and Space Astronomy, Purple Mountain Observatory, Chinese Academy of Sciences, Nanjing 210008, China

Similar results：

Young SNRs

Old SNRs

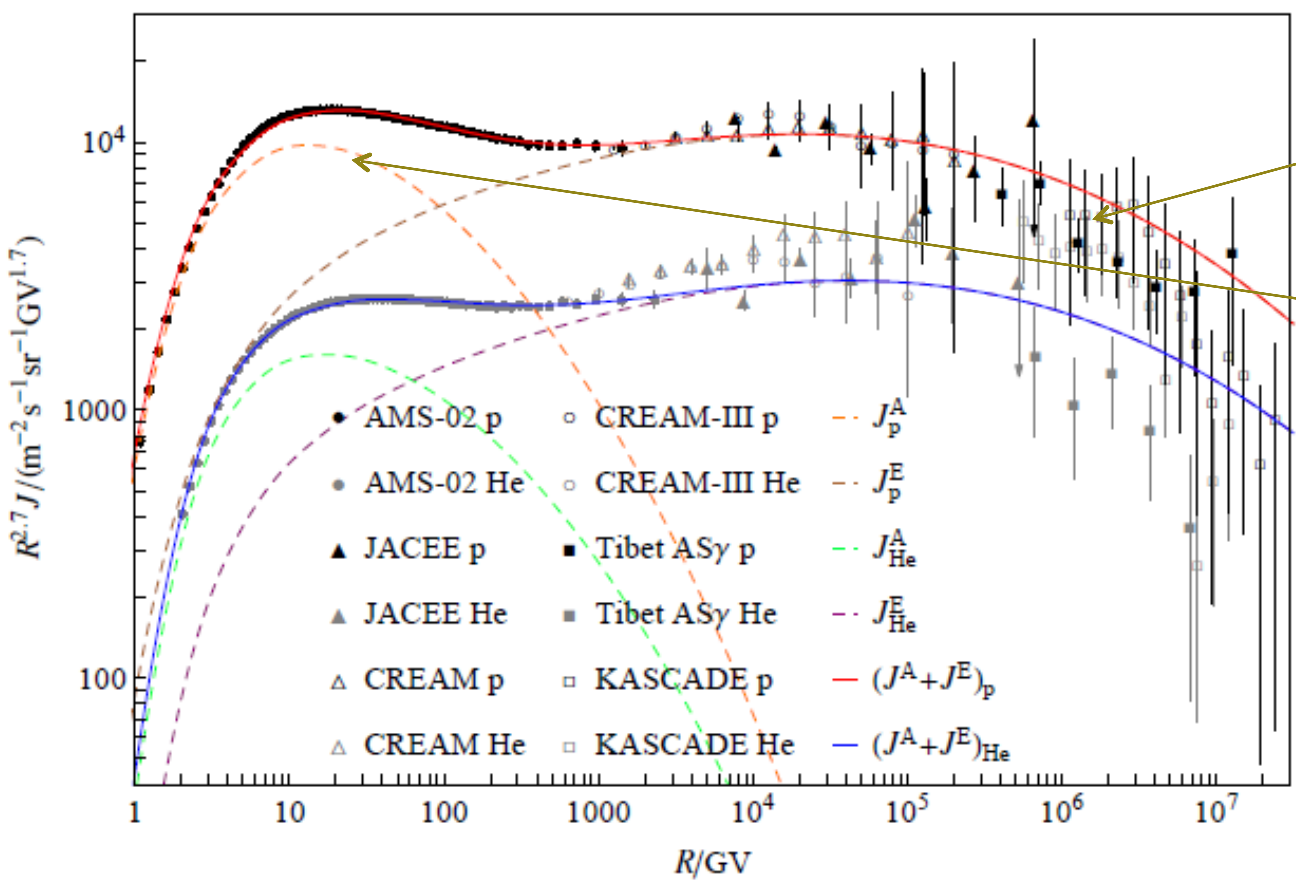

Conclusions

(1)The particle distribution can be described by a broken power-law function with a high-energy cutoff for all SNRs.

(2)The low-energy spectra become harder and the break energy decreases with aging of SNRs,

(3)For most middle-age SNRs, the energy loss timescale of electrons at the high-energy cutoff is approximately equal to the age of the corresponding remnant, implying quenching of high-energy electron acceleration; for young SNRs, this energy loss timescale is shorter than the age of SNRs implying continuous particle acceleration and energy loss limited maximum energy; and for a few old age SNRs, the energy loss timescale are longer than the age of SNRs which may suggest escape of highest energy particles from SNRs.

(4)Our results reveal possible relation between particles distribution in SNR and CRs spectrum and support the SNR origin of galactic CRs

中國科學院紫金山天文台

Purple Mountain Observatory, Chinese Academy of Sciences

Thanks For Your Attention